NATIONAL TECHNICAL UNIVERSITY OF ATHENS
SCHOOL OF NAVAL ARCHITECTURE AND MARINE ENGINEERING
DEPARTMENT OF SHIP DESIGN & MARITIME TRANSPORT

DIPLOMA THESIS

Numerical analysis of the parametric roll resonance of a post-panamax containership in irregular longitudinal seas.

IOANNIS KOUTSOPOULOS

SUPERVISOR: PROFESSOR KONSTANTINOS J. SPYROU

ATHENS
2017

Acknowledgements

This thesis is the final step of my academic studies in the School of Naval Architecture and Marine Engineering of the National Technical University of Athens. The described work on wave groups and the parametric rolling of ships was carried out under the useful guidance and help of my supervisor, Professor K.J. Spyrou, who gave me the chance to deal with one of the challenging topics of modern naval architecture. The support of the doctoral students I. Kontolefas and P. Anastopoulos was of essential importance in order to overpass obstacles during the development of the present thesis. Their assistance was critical for the completion of the thesis. Furthermore, I would like to thank my family for their endless support throughout my studies and through my whole life in general. I owe to my family all my accomplishments so far. Moreover, I would like to thank all my friends and colleagues that supported me in all these years, during difficult situations. Lastly, this thesis is dedicated to the memory of my cousin Michalis who passed away 2 years ago and I hope that through my work I make him proud.

Abstract

The aim of the current thesis is to investigate thoroughly the generation of the phenomenon of parametric rolling that is known to appear for ship hull forms with intense flair and raised stern. The study is an effort to broaden the work of Dousia (2015) in the direction of using more realistic wave profiles encountering the ship. The code that is used in the present thesis is written in the Mathematica environment and includes parts of the code constructed by Kontolefas (2012) for the representation of the ship's hull characteristics and hydrostatics and parts of the code of Dousia (2015) for the calculation of the metacentric height along the wave and the construction of stability charts. Ship rolling is considered as single-degree-of-freedom and the damping term is taken as linear. Numerical studies are conducted for various forms of the wave group and for different wave lengths and number of waves constituting each group, for different loading cases and ship forward speeds, in order to identify areas of instability. Useful conclusions regarding the relation of wave form and forward speed with parametric rolling are made in the final chapter of this thesis.

Περίληψη

Ο σκοπός της παρούσας διπλωματικής εργασίας είναι η λεπτομερής διερεύνηση των κυριότερων παραγόντων που επηρεάζουν την εμφάνιση φαινομένων δυναμικής αστάθειας στα πλοία, όπως για παράδειγμα την παραμετρική αστάθεια. Η εργασία αυτή είναι μια προσπάθεια να διευρύνθει η δουλειά της Ντούσια (2015) προς την κατεύθυνση της θεώρησης του προφίλ των κυματισμών ως ομάδας κυματισμών (wave groups) με διαφορετικού ύψους κύματα κατα μήκος της ομάδας, αντί για την θεώρηση απλών αρμονικών κυματισμών ίδιου ύψους. Ο κώδικας που χρησιμοποιείται είναι γραμμένος σε προγραμματιστικό περιβάλλον Mathematica και περιέχει κομμάτια κώδικα από την εργασία του Κοντολέφα (2012) για την απεικόνηση των χαρακτηριστικών της γάστρας του πλοίου και των υδροστατικών και κομμάτια κώδικα από την διπλωματική της Ντούσια (2015) για τον υπολογισμό του μετακεντρικού ύψους κατα μήκος του κύματος και την κατασκευή των επιθυμητών διαγραμμάτων αστάθειας. Η διαφορική εξίσωση διατοιχισμού που χρησιμοποιείται είναι ενός βαθμού ελευθερίας και ο όρος απόσβεσης θεωρείται γραμμικός. Με αριθμητική ανάλυση των δεδομένων για διάφορες μορφές των θεωρούμενων ομάδων κυματισμών για ένα έυρος τιμών μηκών κύματος και αριθμού κυμάτων στην ομάδα και για διάφορες καταστάσεις φόρτωσης και ταχύτητες του πλοίου έγινε δυνατή η κατασκευή των διαγραμμάτων αστάθειας. Με βάση αυτή εξάγαμε χρήσιμα συμπεράσματα για το φαινόμενο όσο αφορά τη μορφή των κυματισμών αλλά και την επιλογή της κατάλληλης ταχύτητας για την αποφυγή ανεπιθύμητων καταστάσεων ως χρήσιμη πληροφορία για τον καπετάνιο.

Table of Contents

List of figures

1. CHAPTER ONE: INTRODUCTION

Dynamic stability is defined as a ship's ability to resist external heeling forces. It is represented as the amount of energy that is spent for the ship to heel from upright equilibrium position till a specific angle of heel. This energy is calculated as the area under the GZ curve. Capsizing of many ships is associated with loss of stability while sailing in severe seas, due to alteration of restoring moment as a function of the position of the ship on the wave. There are many types of potential dynamic instabilities when a vessel is sailing in longitudinal waves such as: surf-riding, broaching-to, pure loss of stability and parametric roll. This thesis is focused on the topic of parametric rolling. As far it concerns the conditions under which parametric roll can occur the main factors are the following [35]:

- The natural period of roll is equal to approximately twice the wave encounter period.
- The wavelength is of the order of the ship length.
- The wave height exceeds a critical level.
- The roll damping is low.

The geometry of the hull is proved to play an important role too in the development of parametric roll. Ships with bow flare and flat transom are more susceptible to this phenomenon, due to the fact that the waterplane area is changing a lot from wave crest to trough, leading to changing in inertia and finally alterations in stability. Containerships are such ships, so they are prone to this kind of dynamic instability issues. Although well-known phenomenon in the naval architecture for more than 60 years, the need of taking into serious consideration this kind of instability became obvious with the tremendous growth of the number of this type of vessels in the last 30-40 years as seen in Figure 1.1.

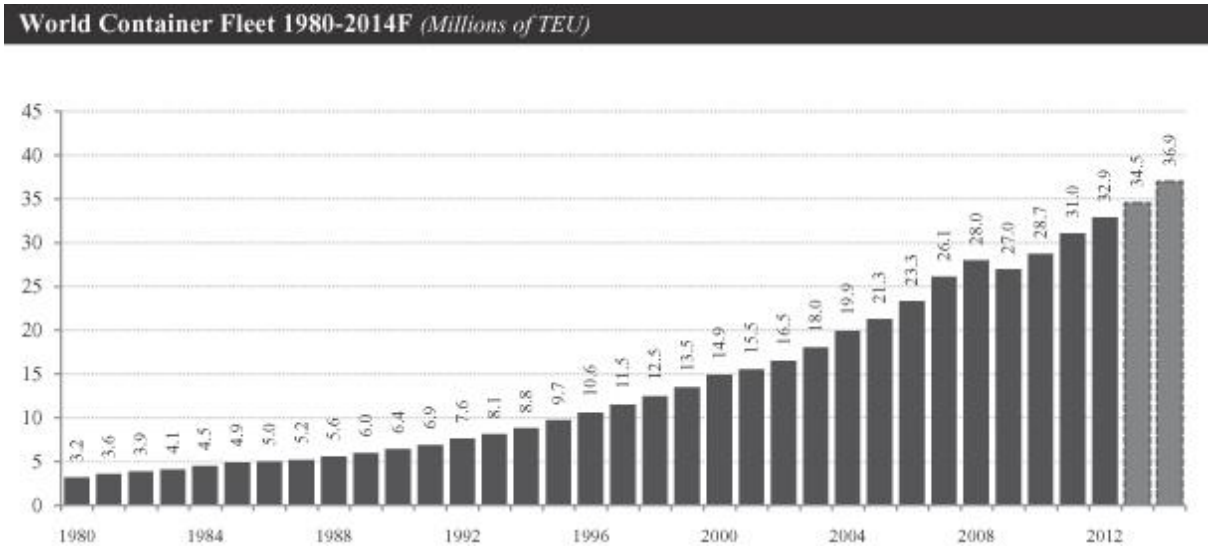

Figure 1.1 Container fleet growth over the last 4 decades [36].

The increasing demand to minimize the delivery time of the cargo, as well as the need for more flexible transportation in the terms of the variety of goods being carried by the same ship, had as a result the wide usage of containerships. Nevertheless, as mentioned earlier, this type of ships is more susceptible to parametric rolling. To prove this in practice there were some reports in the 1990s of containerships experiencing heavy rolling in longitudinal seas, which indicated the potential parametric instability which can occur in this category of vessels. What brought the naval society into action was the so well-known incident of APL China. The paper of France et al. in SNAME's annual meeting in 2001[2] explained the whole accident in detail. In 1998 the post-panamax APL China was en route from Kaohsiung, Taiwan, to Seattle, USA, when she encountered heavy storm in the north Pacific for about 12 hours. The Master decided to reduce speed in order to avoid worse situations. This act did not have a better impact in the ship's stability, the crew of the ship noticed extreme motions in yaw, pitch and roll instead. Especially roll angles exceeded many times 35 degrees and reached up to 40 degrees. After surveillance was carried out the next morning, it was found out that almost 900 containers were lost in sea or damaged and that resulted to a huge financial problem for the company managing the specific ship. The total worth of the damage was estimated about 50 million dollars, which was way more than the value of the entire ship [7]. The magnitude of the devastation can be seen in Figure 1.2. A fundamental part of the ship design process is to ensure stability against capsize. Since then numerous parametric roll-relevant accidents have occurred such as Maersk Carolina(2003), P&O Nedlloyd Genoa (2005) (Figure 1.3), CMA CGM Dahlia (2008) etc. International Maritime Organization (IMO) was really concerned of the fact and from 1995 proposed

guidance to the master in order to avoid parametric resonance in following seas [3]. As a result, the need to include also head seas scenarios into the guidance became obvious and that lead to IMO's revised guidance in 2007 [4]. The new designs used for building vessels with "unconventional" hull characteristics, as well as the need to understand more deep the mechanism under which dynamic instability phenomena occur [1] in order to optimize the operational guidance to the masters, alerted the scientists during the 15 last years. As Peters et al. notes, [5] the absence of scientific background in the existing criteria of IMO is limiting the degree of confidence as new designs come out and as the hull shapes differ quietly from one category to another (e.g. tankers-containerships) [6]. It is of great importance so, to have a general formula which can be used widely for any type and form of the new coming vessels. This is why a process towards the development of second generation criteria is under way. The nonlinearity of GZ curves, in contrary with the assumptions made in the first criteria, and the stochastic nature of the sea waves, and more specific the need to calculate exactly the metacentric height in every position on the wave, require numerical simulations in computers that are computational expensive and difficult to construct. It is mandatory, obviously, the need to have a way to define how metacentric height changes in irregular waves that are closer to reality than regular harmonic waves. Knowing the way GM changes along a wave profile gives more accurate form in the Mathieu equation and so the produced stability charts will be more reliable. The use of numeric method could be helpful in the completion of this purpose.

Figure 1.2 The condition of APL China when reached to US port [37].

Figure 1.3 The P&O Nedlloyd Genoa casualty(2005) [38].

For this reason, our main aim is to numerically calculate the GM variation along irregular sets of waves, and therefore examine the incidents of potential parametric resonance.

The plan of the present thesis is presented below:

- Chapter 2 is a brief literature review on the studies that are associated with parametric resonance phenomena, chronologically ordered from the early observations to more recent studies.
- Chapter 3 describes the goals that are to be accomplished through the completion of the process.
- In Chapter 4, the construction of the under study wave groups may be found, based on the Airy wave theory.
- In Chapter 5, the nature and mathematical background of parametric resonance is introduced, followed up by some numerical simulations. Furthermore, the parametric roll phenomenon is described in detail and the mathematical model that will be used is presented.
- Chapter 6 contains parts of the process that is followed in Kontolefa's [30] thesis for the construction of Mathematica code which calculates the main hydrostatic

factors of the under study ship. In addition parts of the Ntousia's thesis [29] for the satisfaction of the equilibrium of forces and moments in a specific position on the wave, leading to the calculation of GM curves, are included.

- Chapter 7 includes the process that is used to solve the differential roll equation and extract the stability charts.
- In Chapter 8 we may find a set of different applications of the method, along with comparisons between different cases.
- Chapter 9 is the final chapter of the present thesis and presents the final conclusions that came up from the application of the method, as well as some possible topics to be examined in future studies.

2. CHAPTER TWO: LITERATURE REVIEW

2.1 Historical Background

Parametric resonance is a phenomenon the existence of which is known to the scientific community not more than 2 centuries. The first one to deal with this phenomenon was Faraday[8], based on the Chladni's[9] figures of a vibrating surface. Faraday observed oscillations of one frequency being excited by forces of double the frequency of powder which was sprinkled over a square plate while the plate was vibrating. Few years later Melde [10] discovered that a periodic stimulation of a taut string parametrically excites transverse waves in the string when the frequency of change of the tension is about twice the natural frequency of any transverse mode, thus the first approach to the frequency ratio 2:1, speaking of encounter frequency to natural frequency, was made. Mathieu [11], with his infamous differential equation, came to put a mathematical base on the above considerations.

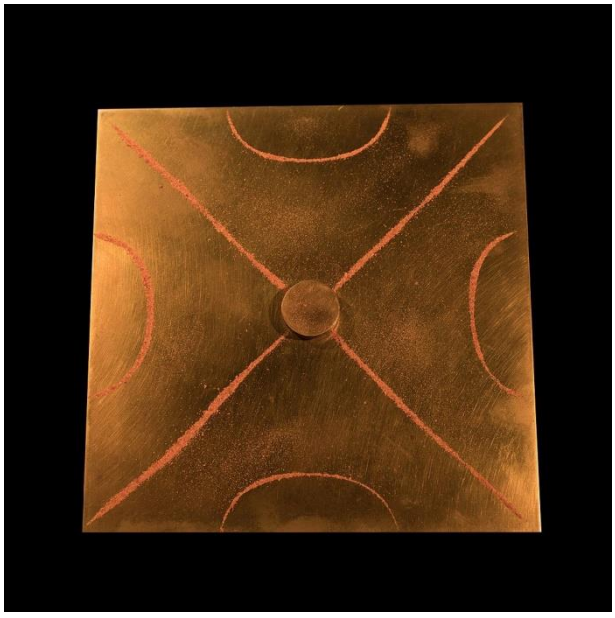

Figure 2.1 Chladni's plate [9]

2.2 Parametric Roll of Ships

The existence of the parametric resonance in ships was firstly observed by Froude [12]. He noted that a ship may have an unfavorable seakeeping behavior in its roll motion, when it is sailing in severe longitudinal waves with natural rolling frequency being half of the natural frequency in heave/pitch. The loss of small fishing vessels in severe following seas and the need to explain these capsizes set the start for more detailed research on this phenomenon in Germany in 1930 [13]. This research included theoretical as well as practical evaluation of the phenomenon in an attempt to be better understood. It was not more than 8 years later, when in 1938 Krempf [14] stated that in following waves a ship has reduced stability when the wave crest is amidships and increased stability when the wave trough is amidships. Graff and Heckscher in 1941[14] strengthened this assumption experimentally. Over the next years the alteration of the differential roll equation to Mathieu-type, as a result of the varying value of the metacentric height in following seas was observed by Grim and Kerwin. Kerwin [14] tried to study the parametric rolling of ships in a single degree of freedom model, while Paulling and Rosenberg[15] took it another step further as they used a three degrees of freedom model in their analysis. Blocki [16] was one of the first to involve the importance of probability to this phenomenon. He introduced the probability of the capsizing of a ship while in parametric roll situation for a given sea state and loading condition, giving useful tools for calculating this probability and establishing preventive methods. Based on the observation by Kempf, Spyrou [17] investigated more deeply the variations of the roll-righting-arm when the ship's position alternates along the wave from crest to trough. This study focused on the approximation of the nonlinearities of damping and restoring, approximated the true GZ curves of a sample containership through polynomials and pointed out the importance of transient responses in the phenomenon, by numerically extracting stability charts.

Although the topic was already known and its nature was under study, parametric roll became top-listed topic among the ship stability related forums with the development and wide use of containerships in the maritime industry. Containerships are vessels with bow flare and flat transom, so they are more susceptible in the appearance of parametric roll. Many containerships reported excessive rolling motions when sailing in longitudinal waves in the early 90s, but the infamous accident of the APL China back in 1998 alerted the scientists to take more serious precautions. France et al. [2] at the SNAME Annual Meeting in 2001 presented a detailed analysis of the incident of the APL China.

The classification societies could not ignore that this phenomenon could result to loss of cargo, loss of ships and, even worse, of human lives. Lloyd's Register [18] set the start in an effort to identify the main aspects that should be taken into account for the limitation of development of parametric resonance in existing ships. It was suggested that two actions could deal with the problem: hull proper modification or increase of the damping coefficient. Because the research was in an early stage and there was not a specific method of decreasing the probability of occurrence of parametric roll, instead Lloyd's' focus turned to the optimization of the container lashing systems, since this concerns containerships widely. The big step was done one year later when ABS in the technical paper of 2004 [19] determined susceptibility criteria and proposed calculation method for the amplitude of parametric roll in longitudinal waves. For the susceptibility criteria a single-degree-of-freedom equation with linear damping was supposed. The alternation of GM within time was assumed to have sinusoidal form and by solving the Mathieu equation, the Ince-Strutt diagrams are extracted. Moreover, the wave encounter frequency and the damping threshold are stated as the two conditions that compose the susceptibility criteria. Last but not least, the effect of the ship's forward speed on the parametric resonance appearance was analyzed in this paper. The weak points of the abovementioned technical paper as well as the need to have a formula to prevent parametric roll from the design stage were outlined one year later in 2005. That was when Spyrou[20] presented "some new ideas about the development of practical design criteria, based on the interfacing of deterministic transient responses with the probabilistic characteristics of wave groups", meaning that there was need the randomness of the real waves to be coupled with deterministic analysis of the ship dynamics. This could be possible if the calculation of the wave height and wave length threshold was based on the deterministic methods and the specification of the probability of encountering a wave of groups with these characteristics was carried out using probabilistic methods. Furthermore, the nonlinearities of the GZ curve and damping and the need of coupling the roll motion with pitch and heave were discussed in that study. Finally, design criteria were proposed in an effort for a more realistic approach on the subject.

In 2007 Spyrou et al.[21] presented a comparative study of the capsize probabilities under parametric roll for an analytical and for a more detailed numerical method(SWAN2), which was not in use until then, testing a post-panamax containership and focusing on the transient response area. For the analytical method, a criterion of the critical magnitude of parametric excitation that is necessary for realizing a roll angle increase from some initial roll disturbance within a limited number of roll cycles is used. Wave groups were used for this

study in an approach to come closer to real sea states. The conclusions of this study were that the analytical method underestimated the probability of encounter of critical wave groups, although it used lower roll damping than the numerical. This was assumed to happen due to the effect of heave and pitch motions to the numerical method. Following this route, Themelis and Spyrou[22] in 2008 conducted a more detailed study of a post-panamax operating in a real sea state in an actual route from Germany to America. The simulation of the sea state was succeeded using the JONSWAP spectrum for the wave group analysis. The meaning of "critical time ratio" was demonstrated in this paper, counting not only the probability of encountering a critical wave group but also taking into account the relevance of the period of the wave group encountered with the period associated with parametric roll resonance. In addition they investigated the role initial conditions could have in the probability of instability and it was concluded that the degree of influence of initial conditions on the overall probability figure depends mainly on the severity of the sea state. Spyrou et al. [23] made a step-by-step evaluation of these susceptibility criteria, which resulted that these analytical descriptions can successfully characterize parametric roll described as a Mathieu-type system, but as the variation of the restoring moment is taken as non-harmonic on waves, more detailed investigation is needed. In this paper it is introduced the method of continuation of nonlinear dynamics in order to achieve a better identification of the stability boundary, and a more reliable prediction of the steady amplitudes of the roll oscillations in parametric resonance. Numerical experiments in irregular oblique seas were carried out by Shigunov et al. [24], who focused on the impact GM variations and forward speed have in the development of the phenomenon, and by Hong et al. [25], who conducted a number of simulations to review the rightness of the susceptibility criteria and to compare the range of wave periods where parametric roll occurs for irregular waves to the periods needed for regular waves. Belenky and Bassler [26] proposed a very useful simplified method of determining the dynamic stability risk in irregular seas in a preliminary stage in 2010. The method treated free surface elevation as a stochastic process, thus considering irregular waves, and took into consideration the average time that the ship's GM would be below a "critical" value. GM calculation was connected straightforwardly to the position along the wave crest and the likelihood of experiencing stability failure was finally expressed as a ratio of the time below this "critical" value and natural roll frequency. The study demonstrated results of this method carried out in many type of vessels, making it applicable for a various range of cases. The same year Silva et al. [27], trying to deal with the avoidance of parametric roll from the designing stage too, published a method to determine the susceptibility of a vessel in extreme roll

angles using the ABS guidelines given in 2004. The method considered a single-degree-of-freedom equation for roll motion in head seas, assumed sinusoidal change of GM along the wave and a regular wave profile. The authors suggested as operational solutions to avoid undesirable roll motions 2 factors: suitable choose of forward speed and appropriate manoeuvrability in order to avoid critical angles of encounter. Many of the results of the numerical simulations came in contrast to what was expected according to susceptibility criteria, thus pointing out the need to review the until then existing guidelines. In a more recent study Rosen et al. [28] gave 3 examples of real incidents connected to principal parametric rolling in following seas, principal parametric rolling in head seas and fundamental parametric rolling in following seas respectively to punctuate the importance and the application of the problem in practice. A multi-degree-of-freedom simulation method was carried out in order to analyze these 3 cases, pointing out operational guidance should follow this direction. In addition, the study reviews the ways that are available in detecting the sea state, which need to be updated in order to predict and avoid unfavorable situations.

3. CHAPTER THREE: THESIS OBJECTIVES

This thesis aims to study thoroughly the issue of parametric roll in containerships and specifically the influence that some principal factors have to the development of the phenomenon in reality. The main objectives of the current study are:

- The theoretical understanding of the mechanism of dynamic loss of stability under which parametric roll occurs.
- The consideration of the wave profile as a height-varying function along the position of the ship on it, rather than a regular harmonic function of strictly sinusoidal shape. Besides, the number of such waves, which form a "wave group", the ship will encounter will be investigated in this thesis. This consideration of irregular waves represents a more realistic approach to the phenomenon, and this reveals the importance of this study which is to examine the effect the variance of the height along the wave and the number of consequent waves the ship passes, in order to extract useful conclusions.
- Numerical calculation of the restoring term GM. The metacentric height in this thesis is not taken as a sinusoidal function or a polynomial approximation, but it is directly calculated numerically in every position the ship is on the irregular wave. For the latter to be done, a numerical code in Mathematica constructed by Kontolefas[30] and further developed by Dousia[29] will be used, in order to have the alteration of GM along the wave, while satisfying equilibrium of forces and moments. The validation of this code using MaxSurf can be found in the thesis of Dousia[29]. Again it is of great interest that the exact numerical calculation of GM is a step towards the direction of more realistic approach, making the results more reliable.
- Input of the previous produced pairs of (x,GMx) in the differential roll equation of a SDOF model as a restoring term. Numerical solutions of the equation led to the construction of the stability charts in each case, which were evaluated and compared for conclusions to be made.

- Further analysis in relation with the ship's forward speed and indication of unfavorable range of speeds for a given wave profile and wave direction[1], for the Master to be well informed of the dangerous speed zones and to avoid parametric roll.

[1] Following or head seas

4. CHAPTER FOUR: WAVE PROFILE CONSTRUCTION

4.1 PROLOGUE

The sea environment is in general a stochastic process and randomness is its principal characteristic. The most common way to describe sea motions is through the surface gravity waves. In an early stage, for simplicity's sake, we will treat surface gravity waves as a harmonic sinusoidal linear function of time and distance. George Biddell Airy [31] made such an assumption like the latter and proposed the next form for the expression of free surface elevation:

$$\eta(x,t) = aCos(kx - \omega t) \qquad (4.1)$$

The definition of each symbol is the following

η is the free surface elevation.

a is the wave amplitude defined as $a=H/2$ with H the wave height.

k is the wave number set as $k=2*\pi/\lambda$ with λ the wave length.

ω is the angular frequency, $\omega=2*\pi/T$ with T the wave period.

The celerity of the wave is known as $c=\lambda/T$.

The graphical display of this function can be seen in Figure 4.1.

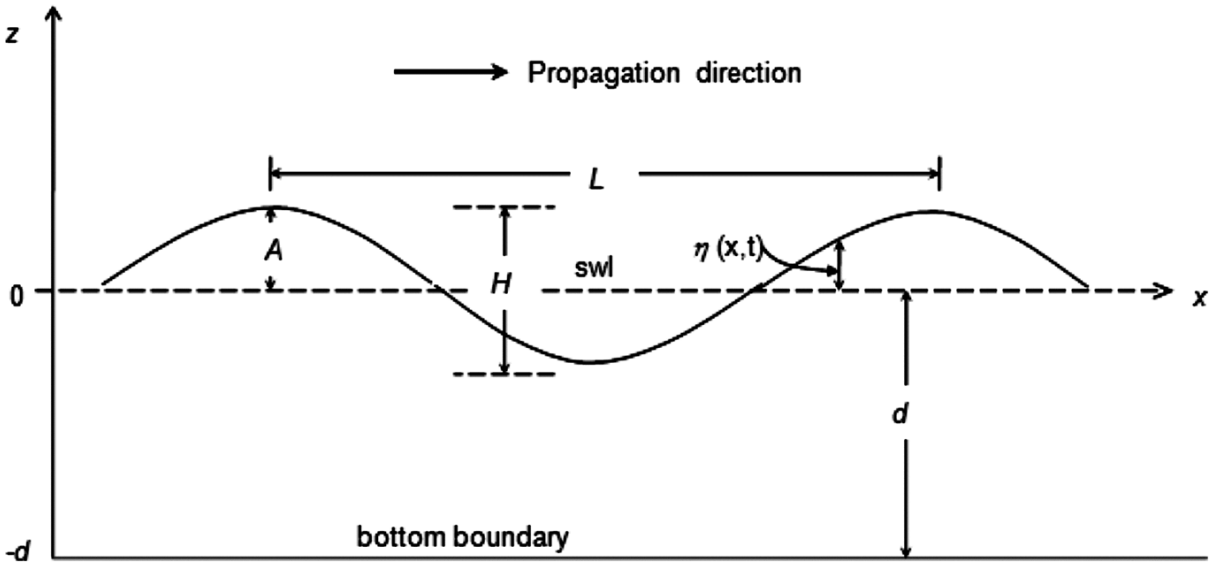

Figure 4.1 Airy wave parameters

4.2 Airy waves physical background

This theory is based on some assumptions which compose the mathematical matrix for the description of the problem. First of all, we consider the fluid (water) to be incompressible and because of the assumption that it does not propagate in the transverse axis-y the equation of continuity for the velocity gives us:

$$\frac{\partial u}{\partial x} + \frac{\partial w}{\partial z} = 0 \tag{4.2}$$

, where u,z the velocity component in the x and z axis respectively.

Secondly the fluid is considered as irrotational, which means that we can replace velocity with velocity potential $u = \frac{\partial \Phi}{\partial x}$, $w = \frac{\partial \Phi}{\partial z}$ and compared to the previous equation we are led to the Laplace equation

$$\frac{\partial^2 \Phi}{\partial x^2} + \frac{\partial^2 \Phi}{\partial z^2} = 0 \tag{4.3}$$

Boundary conditions are needed at the bed and the free surface in order to close the system of equations. We consider the sea bed to be impermeable which leads to the kinematic bed boundary-condition:

$$\frac{\partial \Phi}{\partial z} = 0 \, , at \; z = -d \tag{4.4}$$

At the free surface the vertical motion of the flow has to be equal to the vertical velocity of the free surface in order the parts of the fluid that are in the surface to stay in the surface. This leads to the kinematic free surface boundary condition:

$$\frac{\partial \eta}{\partial t} + u \frac{\partial u}{\partial x} = w \tag{4.5}$$

Bernoulli's equation for an unsteady potential flow gives us the last boundary condition needed to define the problem and is associated with the equality that has to be granted between the pressure on the surface and the atmospheric one. The pressure above the free surface is assumed to be constant. The dynamic free surface boundary condition is defined then as:

$$\frac{\partial \Phi}{\partial t} + \frac{1}{2} v^2 + \frac{P}{\rho} + gz = 0, where \; v = u^2 + w^2 \; and \; z = h \tag{4.6}$$

The associated velocity potential, satisfying the Laplace equation (4.3) in the fluid interior, as well as the kinematic boundary conditions at the free surface (4.4), and bed (4.5), is:

$$\Phi = \frac{\omega}{k} \alpha \frac{\cosh(k(z+h))}{\sinh(kh)} \sin(kx - \omega t) \tag{4.7}$$

If we insert this velocity potential to Bernoulli equation given before we get pressure field,

$$p(x,z,t) = -\rho g z + \rho g \frac{H}{2} \frac{\cosh[k(z+d)]}{\cosh(kd)} \cos(kx - \omega t) \tag{4.8}$$

Last but not least it is of great importance to analyze the dispersion relation. The dispersion relation is defined as,

$$\omega^2 = gktanh(kd) \tag{4.9}$$

And if we replace $\omega=c*\lambda$ and $k=2*\pi/\lambda$ we get

$$c = \pm\sqrt{\frac{g\lambda}{2\pi}\tanh(\frac{2\pi d}{\lambda})} \tag{4.10}$$

The abovementioned is the expression used in the intermediate water region $2<\lambda/d<20$ which will be considered in the terms of this thesis.

4.3 Construction of under study waves

As mentioned earlier, airy waves are a good start to study the sea environment in an early stage, but the consideration of harmonic, fixed-amplitude free surface elevation is far from the reality. In this chapter, we will try to move a step closer to the instances a ship is more likely to encounter during its lifetime. As a first approach, we will examine the amplitude factor in the free surface elevation function. We need to transform the initial expression (4.1) in order to have a distance-varying wave amplitude, assuming that we talk about more than one consecutive waves. If we choose to study a sequence of 7 waves for example, then the free surface elevation as a function of the distance, time fixed, will be as seen in Figure 4.2.

The expression for the free surface elevation for fixed time is:

$$\eta(x) = \frac{H}{2}\cos\left(\frac{2\pi x}{\lambda}\right), where\ \lambda\ the\ wavelength \tag{4.11}$$

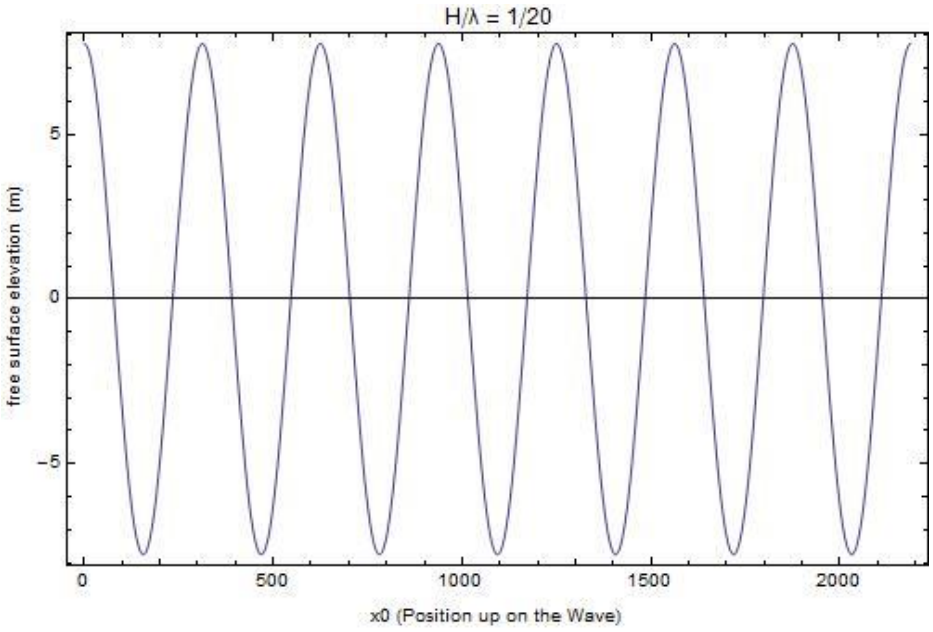

Figure 4.2 Regular waves

As it is obvious, in order to change the amplitude along the whole length of these 7 waves we need to find a formula to insert into the free surface elevation so we get the desirable form. An exponential function is used to accomplish this purpose, thus multiplied by the initial function the result will be alternating amplitude from one wave to another.

The form of the function is

$$g(x) = e^{-ax^2} \tag{4.12}$$

, with a defined as the "filter" parameter which controls the magnitude of the changing. We need furthermore to move this function along the x-axis so its peak is centralized in the middle wave of the wave profile, as discussed before. This will change the expression of $g(x)$, giving us $g(x)=e^{-a(x-\frac{n\lambda}{2})^2}$, where n is the number of the considered waves consisting the group. Finally, we need to make the previous term dimensionless so we divide it by λ^2 and the final expression of the constructed function will be $g(x)=e^{-a\left(x-\frac{n\lambda}{2}\right)^2/\lambda^2}$.

The complete form of the desired expression will be

$$f(x) = \frac{H}{2} e^{-a\left(x-\frac{n\lambda}{2}\right)^2/\lambda^2} \cos\left(\frac{2\pi x}{\lambda}\right) \tag{4.13}$$

Of course it is obvious that for $a=0$ we get the regular wave form, and as the "filter" increases we go to more sharp changes of the amplitude from one wave to another.

An example is given for the two values of $a=0.025$, $a=0.05$ that will be examined in this thesis in the following chapters in Figure 4.3,Figure 4.4.

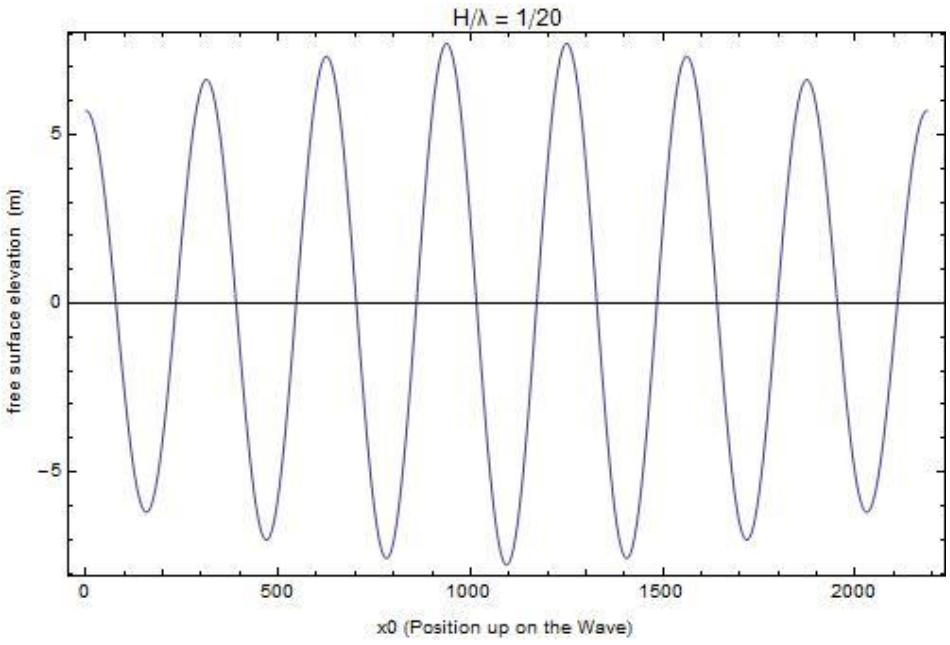

Figure 4.3 Filter parameter=0.025

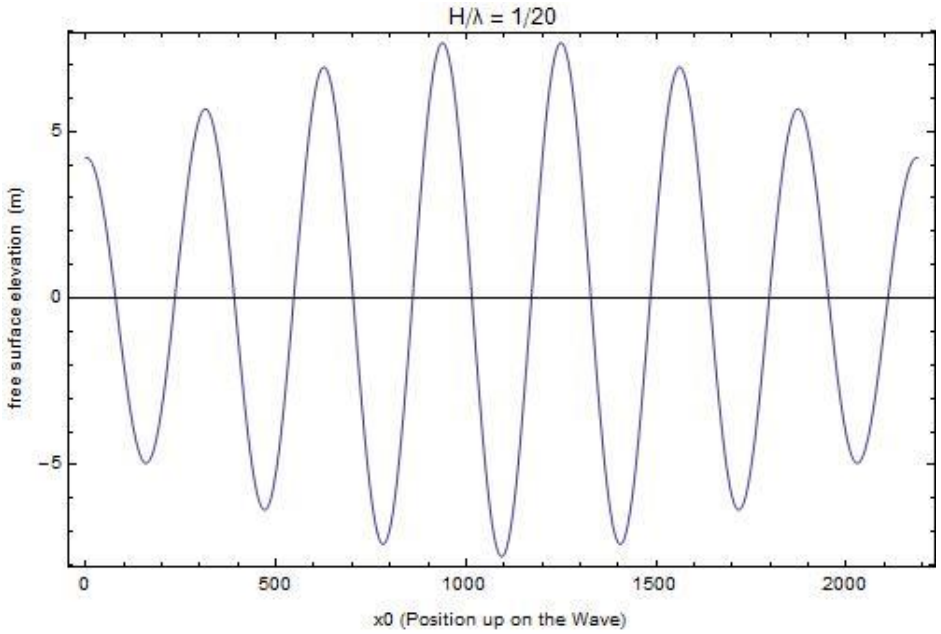

Figure 4.4 Filter parameter=0.05

Comparing the above shown cases we can see the influence the parameter a has in the result in Figure 4.5.

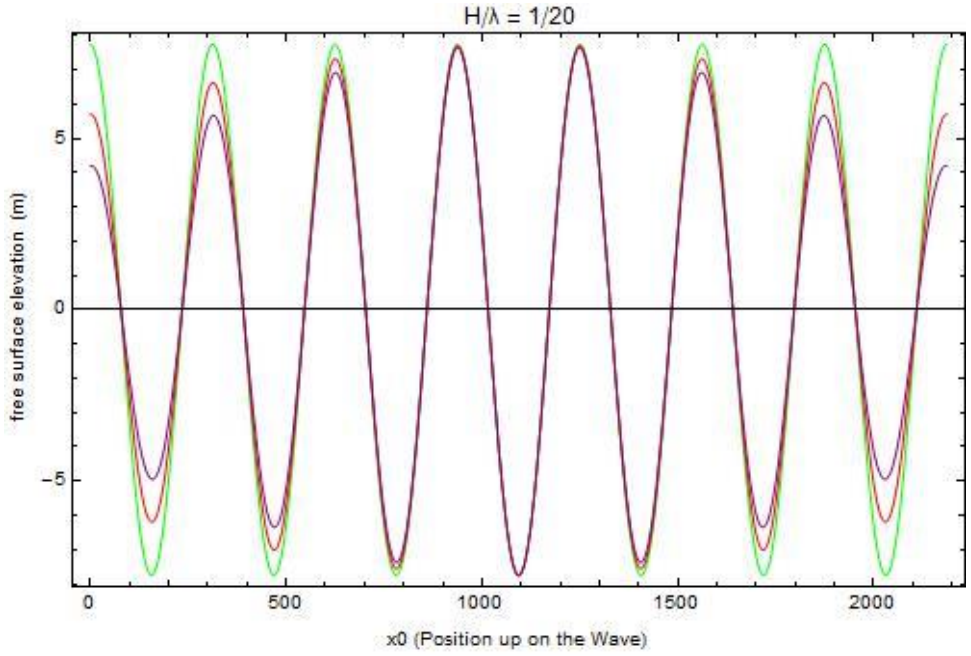

Figure 4.5 Filter parameter's display

As one can see in the Figure 4.5, these three cases do not have the same energy. There is a need so to insert an energy equality condition so the three different forms can be studied under the same energetic basis. We can find an expression of wave energy in Ochi's study [32]:

$$\bar{P} = \lim_{T\to\infty} \frac{1}{2T} \int_{-T}^{T} \{x(t)\}^2 \, dt \, , where \; \bar{P} \; is \; the \; wave \; average \; energy \tag{4.14}$$

In the above expression if we replace time-related terms with distance-related, namely time period T with wavelength λ and time interval with distance interval, and if we assume as reference the energy of the regular wave then by dividing this energy with the other two calculated energies, we get two ratios that when multiplied by these irregular forms will give us the energy equality we need.

After calculation these 3 modified wave forms are shown in Figure 4.6, where the green line represents regular waves (a=0), the red refers to a=0.025 and the purple to a=0.05.

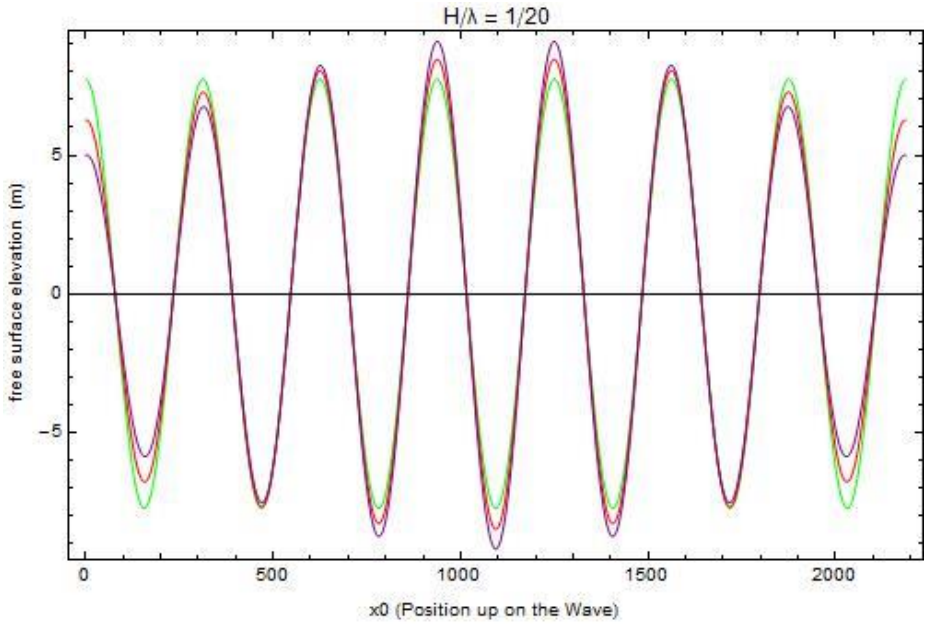

Figure 4.6 Energy balanced waves

5. CHAPTER FIVE: PARAMETRIC RESONANCE

5.1 INTRODUCTION

In this chapter we will investigate the connection between the damped linear differential equation of a SDOF pendulum and the differential roll equation used to describe parametric roll in ships. The main factors that define the phenomenon will be pointed out and the reason why it is difficult to have an analytic solution to the linear Mathieu equation will be discussed.

Supposing that we study a linear damped differential equation of a SDOF pendulum without external force, the expression is given by:

$$\varphi''(t) + b\varphi'(t) + g(t; H, a, \omega)\varphi(t) = 0 \qquad (5.1)$$

Where b is the damping coefficient

$g(t; H, a, \omega) = \frac{H}{2} e^{-at^2} \cos(\omega t)$ *is the restoring term*

We choose to modify the (5.1) into

$$\varphi''(t) + b\varphi'(t) + (1 + g(t; H, a, \omega))\varphi(t) = 0 \qquad (5.2)$$

And furthermore (5.2) into

$$\varphi''(t) + b\varphi'(t) + \omega_o^2\left(1 + \varepsilon e^{-at^2} \cos(\omega t)\right)\varphi(t) = 0 \qquad (5.3)$$

, with w_o the eigenfrequency of the system, $w = 2\pi/T$, T the period of the g, a as mentioned the filter parameter and $\varepsilon = H/\omega_o^2$.

Numerical solutions were conducted in Mathematica for a range of periods between 1 second and 10 seconds, for a range of amplitude between 1 meter and 5 meters with ω_o being comparable with ω. Damping coefficient b is taken as 0.05 and the parameter a took values that could give us sufficient results.

The solutions of the equation (5.3) can be seen in Figure 5.1,Figure 5.2,Figure 5.3.

The shaded areas represent the solutions that exceeded a threshold value of response angle equal to 57 degrees.

It is reminded that $a=0$ stands for restoring term of simple harmonic form.

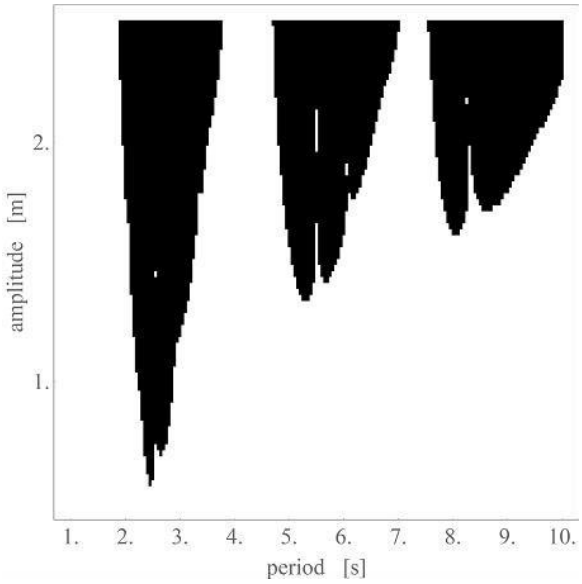

Figure 5.1 a=0

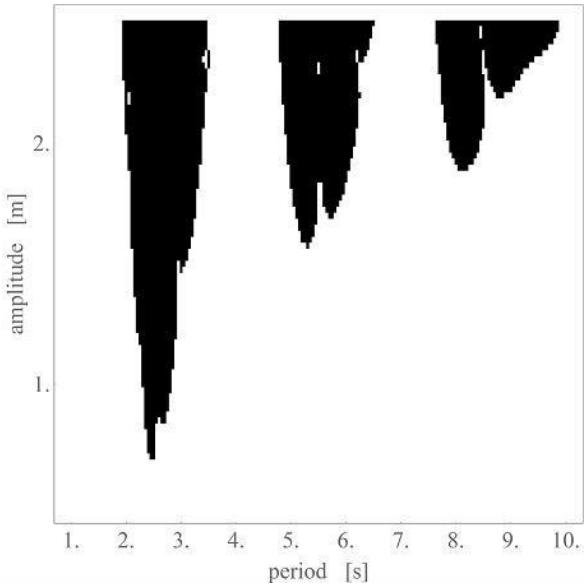

Figure 5.2 a=0.001

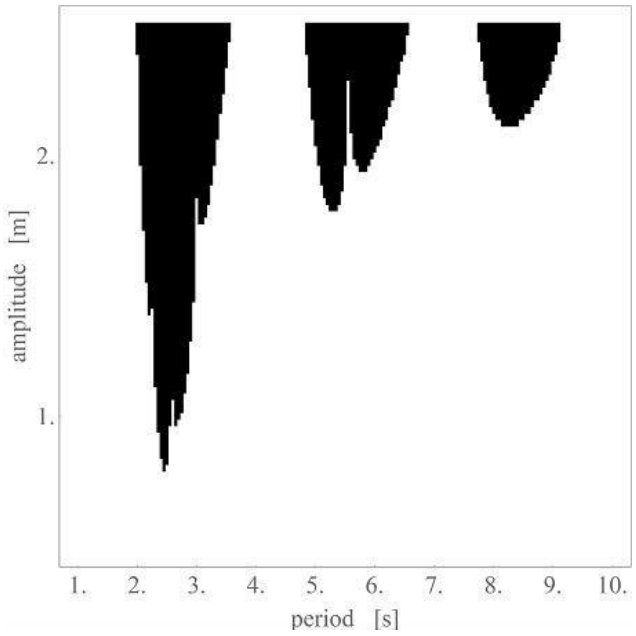

Figure 5.3 a=0.002

From the numerical solutions given by (5.3) we extract the following interesting results:

- We see that the second area starts in a value of period twice the one in the first area, while the third area in a value three times bigger than the first one. A parametric behavior related to parametric rolling is revealed therefore.
- It is obvious from the above figures that while the "filter" parameter a is increasing, leading to non-regular restoring forces, the unfavourable areas tend to decrease. This let us conclude that the regular theoretical form of the g overestimates the probability of parametric resonance in a dynamic system. This will be discussed in detail in a following chapter.

5.2 PARAMETRIC ROLL PHENOMENON

Parametric resonance occurs when the direction of the response of a dynamic system is different from the direction of the exciting force. When a ship is sailing in longitudinal waves, following or head seas, it is expected to response in the heave and pitch motion only. Yet, due to fluctuation of the transverse metacentric height GM along the wave this ship develops roll motions that may lead to unfavourable results such as cargo loss or even worst, capsizing.

As known the metacentric height GM is given as:

$$\mathrm{GM} = \mathrm{KB} + \mathrm{BM} - \mathrm{KG} \tag{5.4}$$

, where KG is the vertical distance of its centroid and depends only on the loading condition of the ship. KB is defined as the vertical distance of the centre of buoyancy and $\mathrm{BM}=\mathrm{I}/\nabla$, with I the second moment of inertia of the waterplane area and V the volume of displacement. During a pass through a wave the ship's waterplane area can change dramatically. Especially for containerships, which have hull geometry with bow flare and small initial metacentric height, this alteration is intensified. This change from the initial waterline in calm water can be seen in Figure 5.4 for a position on a wave crest amidships(a) and on a wave trough amidships(b) respectively.

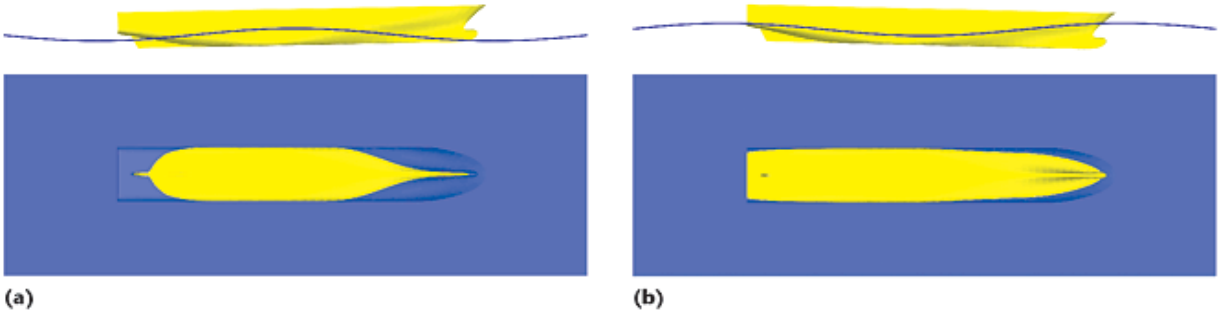

Figure 5.4 Change of waterline from wave crest(a) to trough(b) [40].

Considering the volume of displacement to be constant in a given loading condition, when the wave crest is located amidships then the waterplane area decreases significantly and this leads to a smaller value of BM comparing to the initial one. The vertical centre of buoyancy KB shows a slight increase because the amidships areas of the ship are submerged, but the decrease of BM is greater than that of the increase of KB [14]. Consequently, the expression (5.4) gives us a smaller value of GM, which means that the stability is decreased in a wave crest. For the same reasons when a wave trough is located amidships, the stability is increased.

The abovementioned fluctuation of ship's stability in longitudinal waves can become crucial when combined with some other parameters. The dominant factor is the encounter frequency. When a ship is sailing in head seas and the wave encounter frequency is nearly twice its natural roll frequency then roll angles may tend to increase with time. So, the ratio of frequencies plays an important role. If we set $n=\omega_n/\omega$, where ω_n the natural roll frequency and ω the wave encounter frequency, which defines if we have head or following seas, the values of n can determine the occurrence or not of parametric roll along with other factors. Such factors are the wavelength, which has to be comparable to the ship's length, and the initial GM, which is small for containerships. In Figure 5.5 we can see the development of parametric rolling.

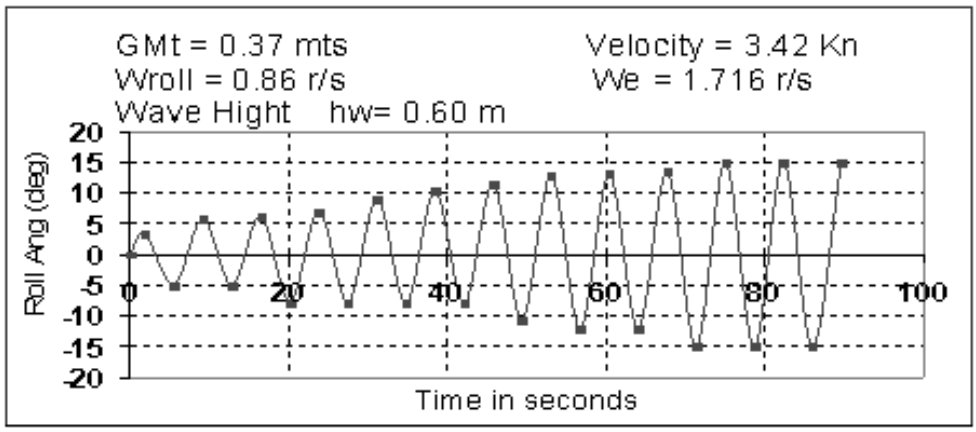

Figure 5.5 Roll angle increase during parametric roll [41].

The mechanism of parametric roll development is best described by the technical paper of ABS [19] and we can see it in Figure 5.6. In this figure the free roll motion in calm water for a given roll disturbance (dotted line) as well as the parametric roll in longitudinal waves for the same initial roll disturbance (continuous line) within time is presented. The alteration of GM values in waves is also shown in the same figure. We can see that after the first quarter period, the roll angle will be slightly larger than it would have been in calm water. At the end of the first quarter of the period, the ship rolls back to the initial, zero degree position but because of its inertia it continues to roll. During the second quarter of the period, the ship encounters a wave crest and the metacentric height tends to decrease and becomes less that the still water value. As a result, the ship rolls to a larger angle than it normally would in calm water with the same roll disturbance, and after the second quarter, the roll angle is increased to a larger value than that at the end of the first quarter. In the third quarter, the ship enters the wave trough and GM becomes greater than the still water value and this leads to resisting the motion. This sequence of GM fluctuation continues periodically as described and this results to greater roll angle values within time.

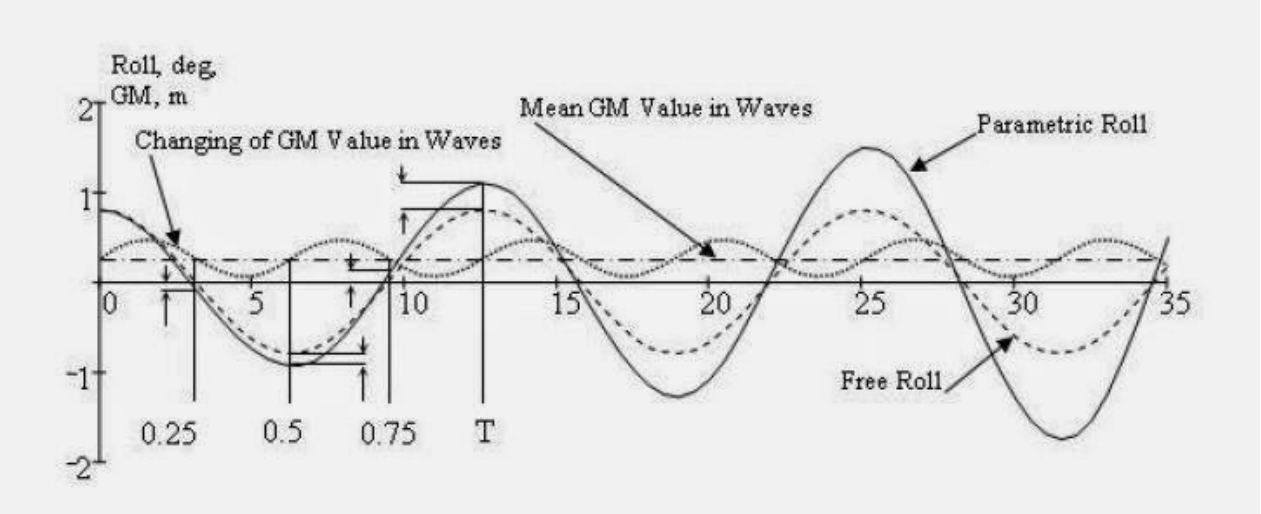

Figure 5.6 Mechanism of parametric roll [19].

5.3 Mathematical model of the problem

In order to examine the phenomenon and find ways to avoid it, we need first to formulate it mathematical and through analysis extract the undesirable conditions. Speaking of parametric roll, as a start we consider the differential equation of roll without the effect of damping and without external stimulation as follows:

$$(I + \Delta I)\frac{\partial^2 \varphi}{\partial t^2} + mgGM(t)\varphi = 0 \qquad (5.5)$$

The restoring term GM(t) is a function of time and a good expression of this function can be found in [14] where GM is considered to change sinusoidally within time and have the form:

$$\mathrm{GM(t)} = GM_0(\,1 + \mathrm{h cos}\omega\mathrm{t}) \qquad (5.6)$$

, where GMo the initial GM in still water, h the fractional variation of GM due to waves, heave and pitch and ω the frequency of encounter the wave.

Inserting the (5.6) into (5.5) we get

$$(I + \Delta I)\frac{\partial^2 \varphi}{\partial t^2} + mgGM_0(1 + \mathrm{h}\cos\omega t)\varphi = 0 \tag{5.7}$$

As is known the roll natural frequency is: $\omega_n{}^2 = \frac{\Delta g G M_O}{I}$,

and by setting $\delta = \frac{\omega_n{}^2}{\omega^2} = \frac{\Delta g G M_O}{I\omega^2}$, and $\varepsilon = \mathrm{h}* \frac{mgGM_O}{I\omega^2} = \mathrm{h}* \frac{\omega_n{}^2}{\omega^2}$,

our expression (5.7) transforms into

$$\varphi''(t) + \omega_n{}^2(1 + \mathrm{h}\cos\omega t)\varphi = 0 \tag{5.8}$$

The (5.8) is the infamous Mathieu equation. Although it has a simple form, it doesn't accept analytical solution, because certain values of the parameter δ do not have stable behavior. The main characteristic of this equation is that the ratio $4*\frac{\omega_n{}^2}{\omega^2} = n^2$, where n any natural number, produces solution which represent unstable region and this can be seen in the diagram of Figure 5.7 which is known as Ince-Strutt diagramm. The non-shaded areas mean that the system is stable, while the shaded represent unstable situations where a small roll disturbance may generate time-increasing roll angles.

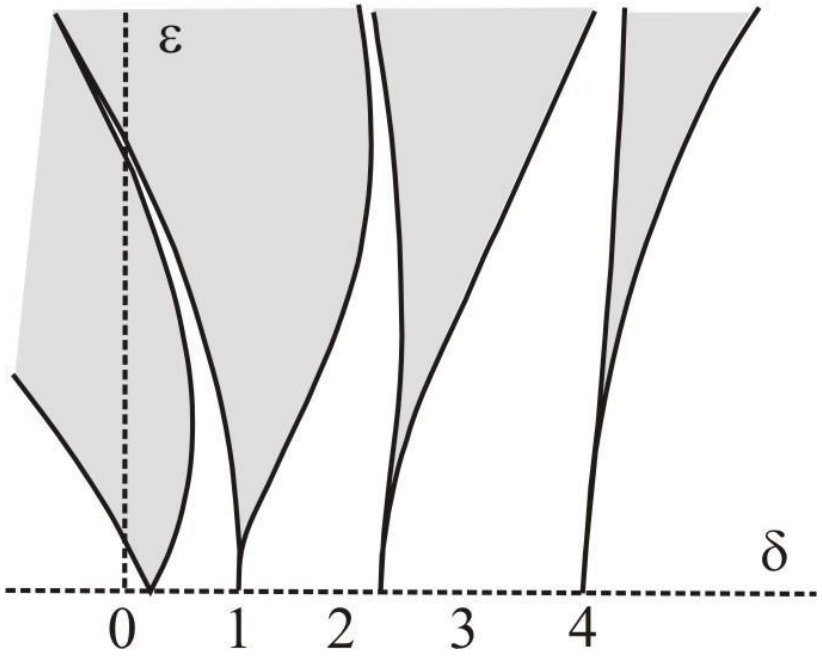

Figure 5.7 Ince-Strutt diagram

Two are the areas of the Figure 5.7 that are applicable to the real ship operation conditions. These areas correspond to values of $4*\frac{{\omega_n}^2}{\omega^2}=n^2$ equal to 1 and to 2, respectively. When the value of n equals to 1, then the phenomenon of principal resonance takes place and then the wave encounter frequency is double the ship's natural roll frequency. When the ratio n is equal to 2, then we fundamental resonance takes place.

The equation (5.8), as discussed before, does not describe the whole phenomenon sufficiently and this is because the effect of roll damping is ignored. Roll damping does not refer to any operational act in order to avoid the development of parametric resonance, but its existence is taken into account in the design process. A ship designed with efficient roll damping has the ability to decay roll motions, as the latter occur as a result of external excitation (e.g. wind,waves). In Figure 5.8 we can see the effect roll damping parameter has in the stabilization of the ship after such excitations take place.

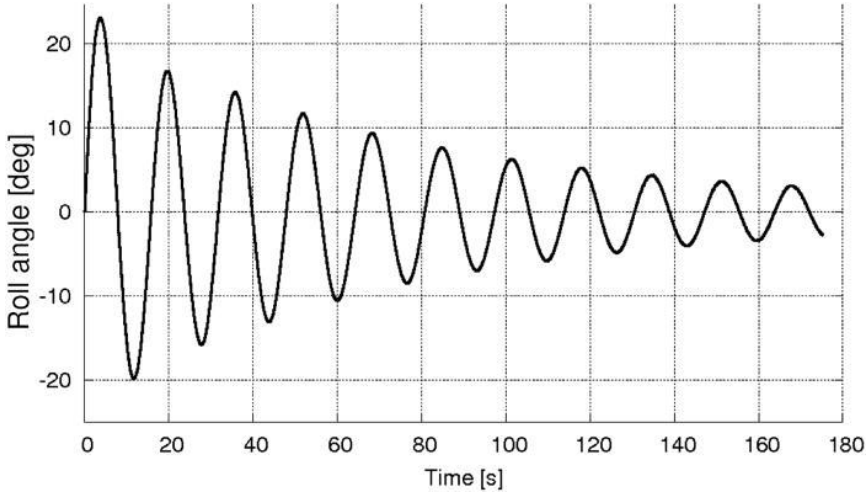

Figure 5.8 Effect of roll damping in the decay of roll motion.

After the damping parameter is included in the (5.8), the expression becomes of the following form:

$$\varphi''(t) + b_1\varphi' + {\omega_n}^2(1 + \mathrm{h}\cos\omega\mathrm{t})\varphi = 0 \qquad (5.9)$$

,where $b_1 = \frac{B_1}{I+\Delta I}$ and B_1 the damping coefficient.

At this point it is important to note the similarity between the expression (5.9) with that one used in the chapter 5.1 (5.3). The main difference lies on the difficulty determining the factor h which is connected with the fluctuation of GM along the wave and will be calculated

numerically in the following chapter. Apart from this, the system discussed in 5.1 and the one used to describe ship's roll in longitudinal waves appear to have quite similar behavior.

In general, roll damping diminishes the probability of unwelcome development of roll angles and, as its value increases, it tends to move the unstable areas upwards in the Ince-Strutt diagrams. This can be easily visually perceived in the Figure 5.9. In this figure, as the roll damping increases, moving from the blue to the green line, the unstable areas are becoming narrower.

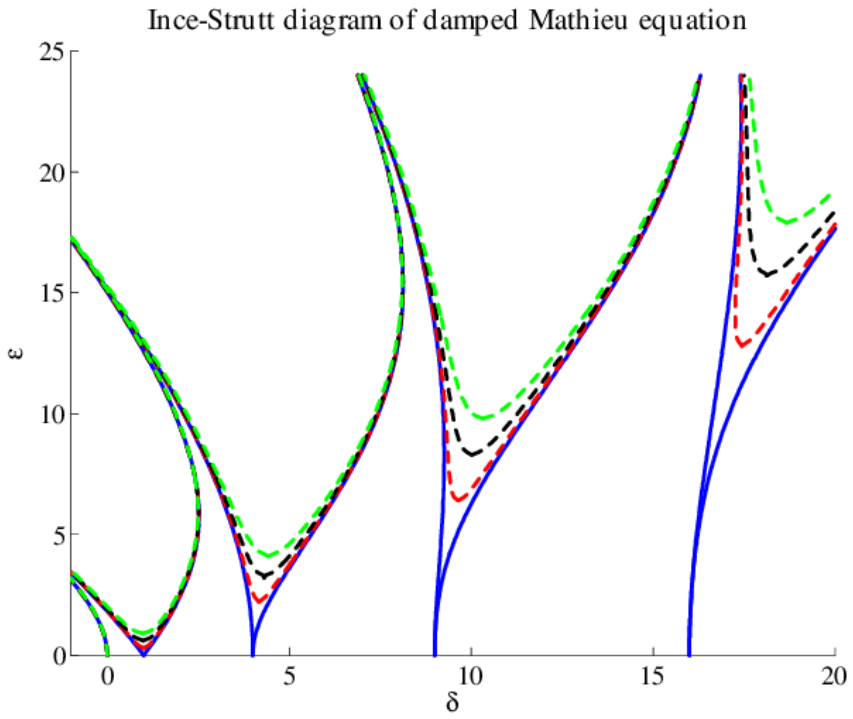

Figure 5.9 Alteration of stability zones due to damping increase [42].

6. CHAPTER SIX: GM CALCULATION

6.1 Introduction

In this chapter we will deal with the calculation of the metacentric height in every position of the ship on the wave in order to be able to solve the differential roll equation and finally produce the desired stability charts. It is necessary to mention that the process that will be followed for this calculation is based on the Mathematica code constructed by Kontolefas[30] for the hydrostatics of a sample ship and further developed by Ntousia[29] for the exact determination of the GM in a selected wave profile, with equilibrium of forces and moments satisfied at any position.

6.2 Axis conventions

Three coordinate systems will be used in this thesis to describe the motion of the free surface, the motion of the ship and the relative motion of the ship up on the wave. These systems are shown in Figure 6.1 [33].

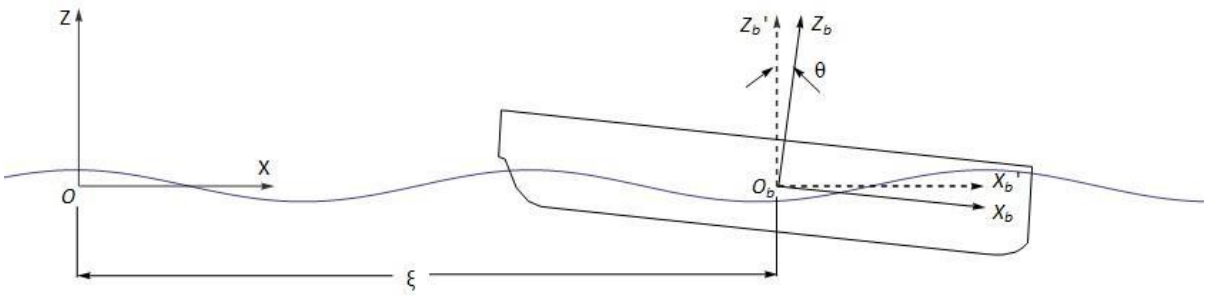

Figure 6.1 Coordinate systems

The first system $O(X,Y,Z)$ is an earth-bound system where the plane (x,y) lies in the still water surface, the positive X-axis is in the direction of the wave propagation and the positive $Z\text{-}axis$ is directed upwards. The second system $O_b(X_b, Y_b, Z_b)$ is a body-bound system which is connected to the ship with its origin at the ship's centre of gravity and follows the motions of the ship. The positive $X_b\text{-}\ axis$ is in the longitudinal forward direction, while the positive $Z_b - axis$ is upwards. The last system $O_b(X_b', Y_b', Z_b')$ is a steadily translating coordinate

system which moves forward with the constant ship speed and is a parallel transfer ξ of the first system.

As we can see from the Figure 6.1, the body-bound system $O_b(X_b, Y_b, Z_b)$ is rotated by an angle, θ, comparing to the system $O_b(X_b', Y_b', Z_b')$ which will be used for the calculations. So we need to transform this system using a rotation matrix A, where

$$A = \begin{bmatrix} cos(-\theta) & sin(-\theta) \\ -sin(-\theta) & cos(-\theta) \end{bmatrix} \tag{6.1}$$

Considering that X_b, Z_b represent the longitudinal and vertical centre of buoyancy LCB and VCB, then

$$\begin{bmatrix} X_b' \\ Z_b' \end{bmatrix} = A \begin{bmatrix} X_b \\ Z_b \end{bmatrix} = \begin{bmatrix} cos(-\theta) & sin(-\theta) \\ -sin(-\theta) & cos(-\theta) \end{bmatrix} \begin{bmatrix} X_b \\ Z_b \end{bmatrix} \tag{6.2}$$

This transformation gives us an expression for the coordinates of centre of buoyancy referring to the moving system as,

$$LCB' = LCBcos\theta - VCBsin\theta \tag{6.3}$$

Accordingly, if we talk about the longitudinal and vertical centre of gravity of the ship LCG and VCG, then

$$LCG' = LCGcos\theta - VCGsin\theta \tag{6.4}$$

6.3 Ship's hull characteristics

In order to examine the behavior of the ship on the wave profile we need first to define the geometry of its hull. For a given set of points *(x,y,z)* for each section, which refer to longitudinal distance from a reference point, semi-breadth and vertical distance from ship's bottom respectively, we are able to get the sectional area and its centroid for all sections. Firstly, this set is inserted into the Mathematica code constructed by Kontolefas and, for a specific local draft for each section, through interpolation up to the before mentioned draft we obtain the sectional area for each station $S(i,T)$ and the centroid of the sectional area $Z_c(i,T)$ which will be used later for the equilibrium of forces and moments. The use of trapezoidal as well as Simpson's method subroutines in the code will help us integrate these sectional areas and centroids in the full length of the hull and obtain, as will be discussed below, the ship's submerged hull volume (∇), longitudinal center of buoyancy *(LCB)* and vertical center of buoyancy *(VCB)*.

The ship's submerged hull volume is given from the expression

$$\nabla = \iiint_{\nabla} dX_p\, dY_p\, dZ_p = \int_{-L/2}^{L/2} dX_p \iint_{S} dY_p\, dZ_p = \int_{-L/2}^{L/2} S(X_p)\, dX_p \tag{6.5}$$

, where $S(X_p)$ is the sectional area of a section in the position X_p with respect to the body-bound system.

The relations for the LCB and VCB can be found from Tzampiras [34] as,

$$LCB = \frac{M_{yz}}{\nabla} = \frac{\iiint_{\nabla} X_p\, d\nabla}{\nabla} \tag{6.6}$$

$$VCB = \frac{M_{xz}}{\nabla} = \frac{\iiint_{\nabla} Z_p\, d\nabla}{\nabla} \tag{6.7}$$

The above expressions (6.6),(6.7) also refer to the body-bound system.

It is essential to note that $S(i,T), Z_c(i,T)$ depend directly on the local draft each section i has when the ship is positioned on the wave. Of course this draft is different from that one in calm water, due to the free surface elevation and the sinkage (heave) of the ship in order to have equilibrium. These local drafts in each section are defined as:

$$T_p = T + Z_p + t \tag{6.8}$$

Where T is the draft of the section in calm water, Z_p is the free surface elevation in the position X_p, according to the body-bound system $O_b(X_b, Y_b, Z_b)$ and t is the heave of the ship and it is considered positive if we have immersion and negative if we have elevation.

In order to calculate the local draft of each section T_p, we need to use the same reference system for all factor of (6.8). The expression of the free surface elevation is given with respect to the earth-bound system $O(X,Y,Z)$, so we need to transform it to the body-bound as mentioned above. To do so we need again to use the rotation matrix inversed this time as follows

$$\begin{bmatrix} X_p \\ Z_p \end{bmatrix} = \begin{bmatrix} cos(-\theta) & sin(\theta) \\ -sin(\theta) & cos(-\theta) \end{bmatrix} \begin{bmatrix} X_p' \\ Z_p' \end{bmatrix} \tag{6.9}$$

And so by analyzing this matrix we get

$$X_p = X_p' cos\theta + Z_p' sin\theta \tag{6.10}$$

$$Z_p = -X_p' sin\theta + Z_p' cos\theta \tag{6.11}$$

The required Z_p is the result of the solution of the system (6.10),(6.11). Firstly, the (6.10) is solved to find X_p', with X_p known and Z_p' is the free surface elevation according to the moving system $O_b(X_b', Y_b', Z_b')$, which compared to the earth-bound system is calculated as $\eta(\xi+X_p')$. The value of X_p' that came of the solution of (6.10), is inserted as input in (6.11) and finally we get the requested result.

6.4 Equilibrium of forces and moments

It is known that for a ship to float up on a wave 2 conditions must always be satisfied, equilibrium of forces and equilibrium of moments in every position at any time.

These two conditions are written as:

$$B = \Delta \tag{6.12}$$

$$B * LCB = \Delta * LCG \tag{6.13}$$

Because the calculations will be made using the moving system $O_b(X_b', Y_b', Z_b')$ the expression (6.13) transforms into the following:

$$B * LCB' = \Delta * LCG' \tag{6.14}$$

It is mentioned that B is the buoyant force and Δ is the ship's displacement.

For a given loading condition the ship's displacement is known and the buoyant force is calculated as $B=\rho g\nabla$,with ρ the fluid's density and g the acceleration of gravity. By making use of the (6.5) for the submerged hull volume the (6.12) is finally written as

$$\Delta = \rho g \int_{-L/2}^{L/2} S(X_p)\, dX_p \tag{6.15}$$

By replacing the terms of (6.6),(6.7) into the expression (6.3) we get

$$LCB' = \frac{\iiint_{\nabla} X_p\, d\nabla}{\nabla} cos\theta - \frac{\iiint_{\nabla} Z_p\, d\nabla}{\nabla} sin\theta \tag{6.16}$$

The integrals included in (6.16) are calculated as

$$\iiint_{\nabla} X_p \, d\nabla = \int_{-L/2}^{L/2} X_p \, dX_p \iint_{S_p} dY_p \, dZ_p = \int_{-L/2}^{L/2} X_p S(X_p) \, dX_p \tag{6.17}$$

$$\iiint_{\nabla} Z_p \, d\nabla = \int_{-L/2}^{L/2} Z_p \, dX_p \iint_{S_p} dY_p \, dZ_p = \int_{-L/2}^{L/2} Z_p(X_p) S(X_p) \, dX_p \tag{6.18}$$

Combining (6.17),(6.18) with (6.5) the (6.16) takes the following form:

$$LCB' = \frac{\int_{-L/2}^{L/2} X_p S(X_p) \, dX_p}{\int_{-L/2}^{L/2} S(X_p) \, dX_p} cos\theta - \frac{\int_{-L/2}^{L/2} Z_p(X_p) S(X_p) \, dX_p}{\int_{-L/2}^{L/2} S(X_p) \, dX_p} sin\theta \tag{6.19}$$

If the condition (6.12) is satisfied, meaning that we have equilibrium of forces, the second condition (6.14) for the equilibrium of moments becomes,

$$B * LCB' = \Delta * LCG' \rightarrow$$

$$cos\theta \frac{\int_{-L/2}^{L/2} X_p S(X_p) \, dX_p}{\int_{-L/2}^{L/2} S(X_p) \, dX_p} - sin\theta \frac{\int_{-\frac{L}{2}}^{\frac{L}{2}} Z_p(X_p) S(X_p) \, dX_p}{\int_{-\frac{L}{2}}^{\frac{L}{2}} S(X_p) \, dX_p} = LCG cos\theta - VCG sin\theta \tag{6.20}$$

The system of equations (6.15),(6.20) defines fully the problem of equilibrium of the ship on a position on the wave.

6.5 Process of GM calculation

The problem of satisfying equilibrium of forces and moments in every position of the ship on the wave is composed by the expressions (6.15),(6.20). As we can see the angle of trim θ as well as the heave τ of the ship will define exactly its position in order to achieve this equilibrium. To do so the numeric code created by Dousia[29] in Mathematica uses a step by step bisection method which for a given position of the reference point of the ship along a wave solves the system of equilibrium of forces and moments for a range of heave $\tau = [\tau_\alpha, \tau_\beta] \in [-H/2, H/2]$ and angles $\theta = [\theta_\alpha, \theta_\beta] \in [-H\pi/\lambda, H\pi/\lambda]$, starting from the values

$(\tau_\alpha, \tau_\beta)$, $(\theta_\alpha, \theta_\beta)$ so that they give results of different sign, and in every step dividing the interval of heave and angle in two by computing the midpoints $\tau_c = \frac{\tau_\alpha + \tau_\beta}{2}$, $\theta_c = \frac{\theta_\alpha + \theta_\beta}{2}$ and continuing this sequence until we find the value of τ_c, θ_c that satisfy the (6.15),(6.20). These values define fully the trim and heave the ship will have in a specific position on the wave in order to float.

Heave and trim will change the longitudinal position of the ship on the wave and, thanks to geometry, the final position is found as:

$$x_f = x_o + \tau_c sin\theta_c \tag{6.21}$$

In this position we calculate the vertical center of buoyancy VCB_x and the local beam in each section corresponding to the local drafts, as discussed before, b_{x_i} will lead us to calculate the second moment of area of the waterplane as

$$I_t = \frac{2}{3} \int_{-L/2}^{L/2} {b_{x_i}}^3 \, dx \tag{6.22}$$

The result of (6.22) will define the value of BM_x because $BM_x = I_t/\nabla$ and, knowing that KG is constant, GM will be:

$$GM_x = VCB_x + BM_x - \mathrm{KG} \tag{6.23}$$

Several solutions of the abovementioned system will give us the pairs (x, GM_x) in the whole length of a sequence of 7 waves for example, as these were introduced in chapter 4. These pairs are forming curves and, for a variety of wave steepness for the waveforms discussed in chapter four, these curves are shown in the following figures. The data of the post-panamax containership that is used for this numerical analysis can be found on the Table 6.1.

Length overall	250.000 m
Length between perpendiculars	238.350 m
Breadth (moulded)	37.300 m
Depth (moulded)	19.600 m
Design draught (moulded)	11.500 m
Freeboard draught (moulded)	12.500 m
Displacement at Td = 11.500 m	68014 t
Displacement at Tfrb = 12.500 m	75729 t

Table 6.1 Ship's main particulars

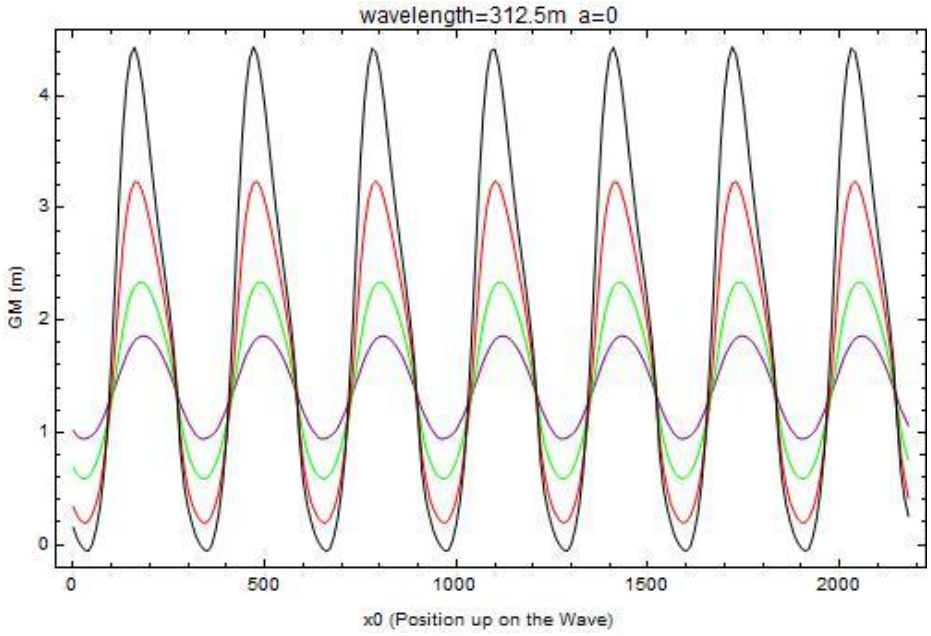

Figure 6.2 Alteration of GM curves along the wave as the wave steepness increases for a=0 regular waves.

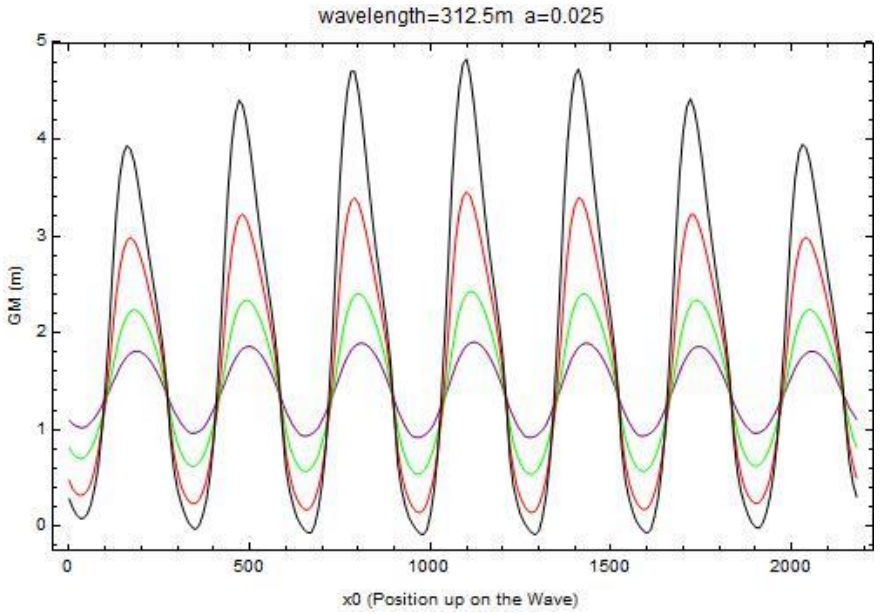

Figure 6.3 Alteration of GM curves along the wave as the wave steepness increases for a=0.025.

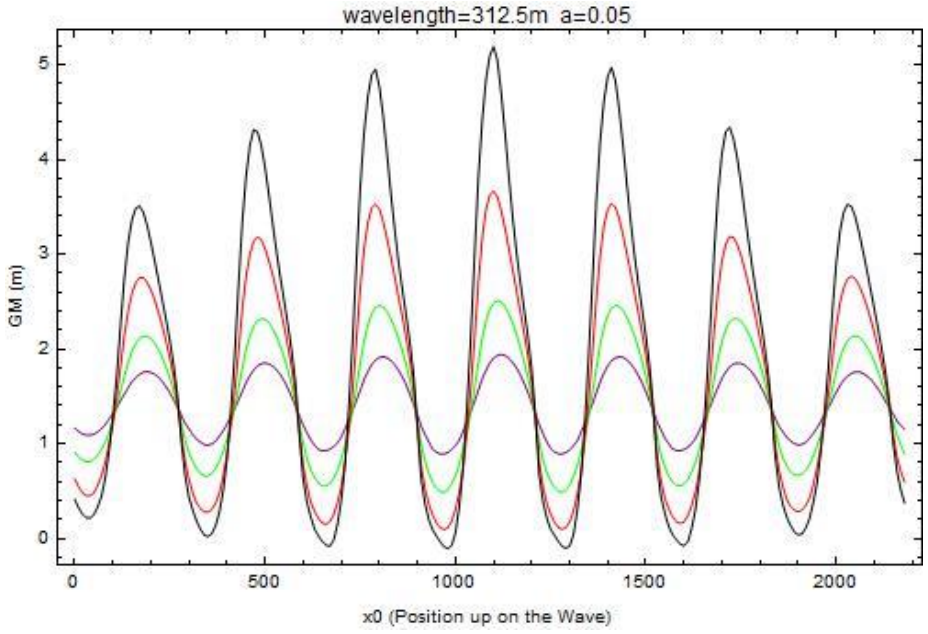

Figure 6.4 Alteration of GM curves along the wave as the wave steepness increases for a=0.05.

7. CHAPTER SEVEN: STABILITY CHARTS

7.1 Solution of roll differential equation procedure

The depiction of the safe and the dangerous conditions a ship may encounter during its lifetime, as far as it concerns parametric rolling occurrence, is possible through the stability charts. These charts are the result of numerous solutions of the equation

$$\ddot{\varphi}(t) + b_1\dot{\varphi}(t) + \frac{mg}{I_x}GM(t)\varphi(t) = 0 \qquad (7.1)$$

The solution of the previous expression gives us the roll angle (φ) alteration within time while a ship encounters a sequence of. The equation will be solved for a range of encounter frequencies and for a range of wave steepness. Every time a response passes a predetermined threshold value of roll angle, then it will be marked as unacceptable because the roll angles will tend to increase within time. The stability chart has as horizontal axis the ratio $a = 4\frac{{\omega_n}^2}{\omega^2}$, where ω_n the natural rolling frequency of the ship and ω the wave encounter frequency. The vertical axis is the wave steepness (H/λ), where H the wave height and λ the wavelength. The (7.1) will be solved for a range of a$\in [0,6]$, because this is the range of frequencies that correspond to real situations a ship may encounter, and for a range of wave steepness that refer to real ocean waves characteristics, meaning a maximum value of H/λ around 0.05-0.06. There solutions will either increase within time, or decrease leading to bounded solutions. In Figure 7.1 we can see as marked blue points the pairs of (a,H/λ) for which the solution of (7.1) exceeds the threshold value. Every factor that is included in the calculation of (7.1) will be analyzed in detail in this chapter.

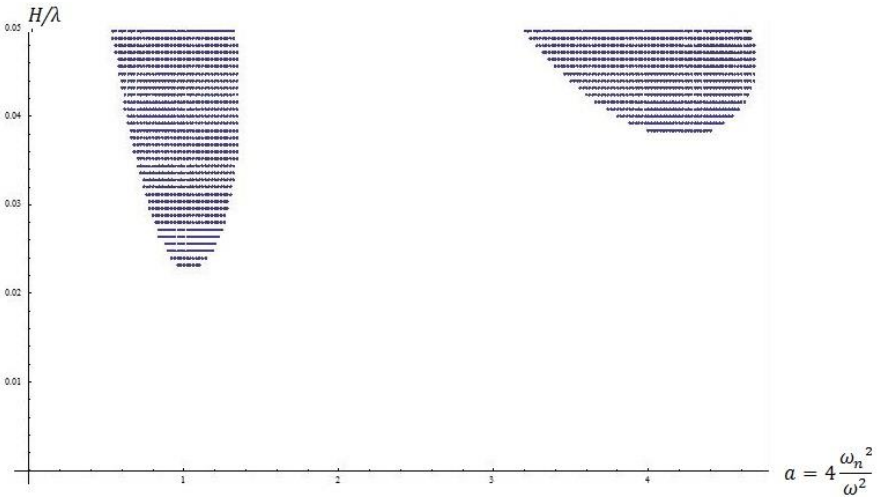

Figure 7.1 Typical stability chart

7.2 Definition of each term

In this paragraph we will deal with every factor included (7.1) and give a formula to calculate them. It is noted that many terms are not distinct but are included in the calculation of some other.

First of all, the term $b_1 = {}^{B_1}/_{I_x}$ where B_1 is given by Spyrou [17] as:

$$B_1 = \frac{2\zeta}{\sqrt{\Delta g I_x G M_o}} \tag{7.2}$$

The factor ζ is around 0.04-0.09 [26].

Because the initial GM_o in still water is given to us in the loading manual, we can calculate the natural rolling period of the system through the expression given by the IMO [3] as:

$$T_R = \frac{2CB}{\sqrt{GM_o}} \tag{7.3}$$

The coefficient C is calculated by the following formula

$$C = 0.373 + 0.023(B/d) - 0.043(L/100) \quad (7.4)$$

Where B is the ship's breadth, d the ship's draught and L is the length between perpendiculars.

The natural rolling period as defined in (7.3) will lead to the calculation of the natural roll frequency as

$$\omega_n = \frac{2\pi}{T_R} \quad (7.5)$$

In chapter (5.3) we had an expression for the natural roll frequency

$$\omega_n{}^2 = \frac{mgGM_O}{I_x} \quad (7.6)$$

If we combine (7.5),(7.6) we get the mass moment of inertia plus the added mass

$$I_x = \frac{mgGM_O}{\omega_n{}^2} = \frac{T_R{}^2 mgGM_O}{4\pi^2} \quad (7.7)$$

The only factor of (7.1) which remains undetermined is the GM alteration within time. In chapter 6 we dealt with the calculation of the metacentric height along a wave or a sequence of waves. As a result we extracted pairs of (x, GM_x) which means that we have distance-dependent values of GM. In (7.1) metacentric height is shown to be time dependent function though, forcing us to make a transformation from distance domain to time domain.

This transformation is possible through the assumption of constant speed of the ship U.

Then, by assuming that the initial position of the ship on the wave is x_o and that the amount of time of wave encounter is t, we can find the position of the ship on the wave as:

$$x = xo + V\,t \tag{7.8}$$

The velocity V that is displayed into (7.8) differs from the ship's constant forward speed and is a relative speed between the one that the ship has and the wave celerity. In order to understand this term better let us consider the reference system shown in Figure 7.2.

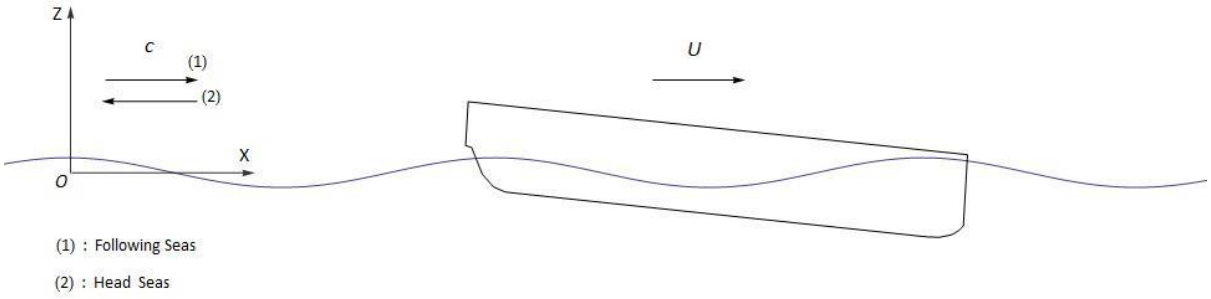

Figure 7.2 Reference system

We consider that the reference system moves along the wave and follows the motion of the ship. The speed of the reference system is the subtraction of the ship's speed and the wave celerity:

$$V = U - c \tag{7.9}$$

The total amount of time that we consider that the ship needs to pass a wave or a sequence of n waves is

$$t = n\frac{2\pi}{\omega} \tag{7.10}$$

,where n is the number of waves consisting the wave group and ω the wave encounter frequency. This means that the ship will reach the position x_i on the wave in the time t_i with the time to be found inside the interval $t_i \in [0, n\frac{2\pi}{\omega}]$. By inserting (7.9),(7.10) into the (7.8), we are able to transform straightforwardly the pairs of (x, GM_x) into pairs of (t, GM_t) which is essential in order to solve (7.1).

At this point it is necessary to define the wave encounter frequency ω which enters in the calculation of the time (7.10) and is the critical factor to determine the ship's forward speed. As discussed in 7.1, we will choose the range of a that will be examined in this thesis and because a is expressed as

$$a = 4\frac{{\omega_n}^2}{\omega^2} \tag{7.11}$$

It is known that ω_n is given by (7.5), which means that the wave encounter frequency is totally described by the requirements set by us. As far as it concerns the speed of the vessel, it is another variable that needs to be set as a function of the wave encounter frequency. The relation given by Peters et al. [5] is as follows:

$$\omega_e = \omega_w - \frac{{\omega_w}^2}{g}Ucos\beta = \frac{\sqrt{2\pi}}{\lambda}(\sqrt{\lambda g} - U\sqrt{2\pi}cos\beta) \tag{7.12}$$

,where U is the forward speed, β is heading angle relative to the waves (0° is following seas and 180° for head), g is the acceleration due to gravity, ω_w is the true frequency of the wave and λ is the wave length.

It is easy to notice that (7.12) can be rewritten as

$$\omega_e = k(c - Ucos\beta) \tag{7.13}$$

And because the unknown to our problem is the forward speed from (7.13)

$$U = (c - \frac{\omega_e}{k})/cos\beta \tag{7.14}$$

With $cos\beta = 1$ for following seas, or $cos\beta = -1$ for head seas

For simplicity's sake, we consider that $cos\beta = 1$, which means $U = (c - \frac{\omega_e}{k})$ and if the result gives us positive value it means that the assumption is right and we have following waves, otherwise we have head seas.

Now that all terms included in (7.1) are calculated, we can proceed to the solution of this equation in Mathematica environment. The alteration of metacentric height along the waves is analyzed in previous chapters and the extracted pairs of (x, GM_x) will give us, through interpolation between many values of wave steepness, the surface shown in Figure 7.3. It is noted that the horizontal axis which refers to the position of the ship on the wave is dimensionless as $x' = \frac{x}{n\lambda}$.

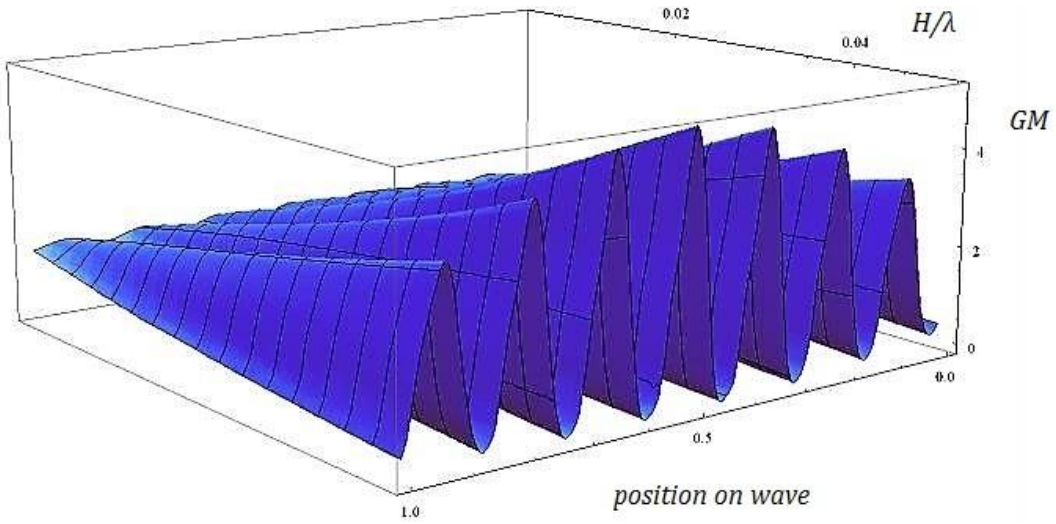

Figure 7.3 GM variation along the wave group of 7 waves for filter parameter=0.05 for many values of wave steepness. The surface is created through linear interpolation.

The initial conditions we need to solve the equation are the following:

$$\varphi(t=0)=\frac{\pi}{180}\,,\dot{\varphi}(t=0)=0 \tag{7.15}$$

The considered threshold value is 0.3[2] and the damping ζ shown in (7.2) is taken as 0.05. Since the problem is well defined, we solve it numerically in Mathematica for a range of $a\in[0,6]$ and wave steepness $H/\lambda\in[0.002,0.05]$. The results can be seen in Figure 7.4.

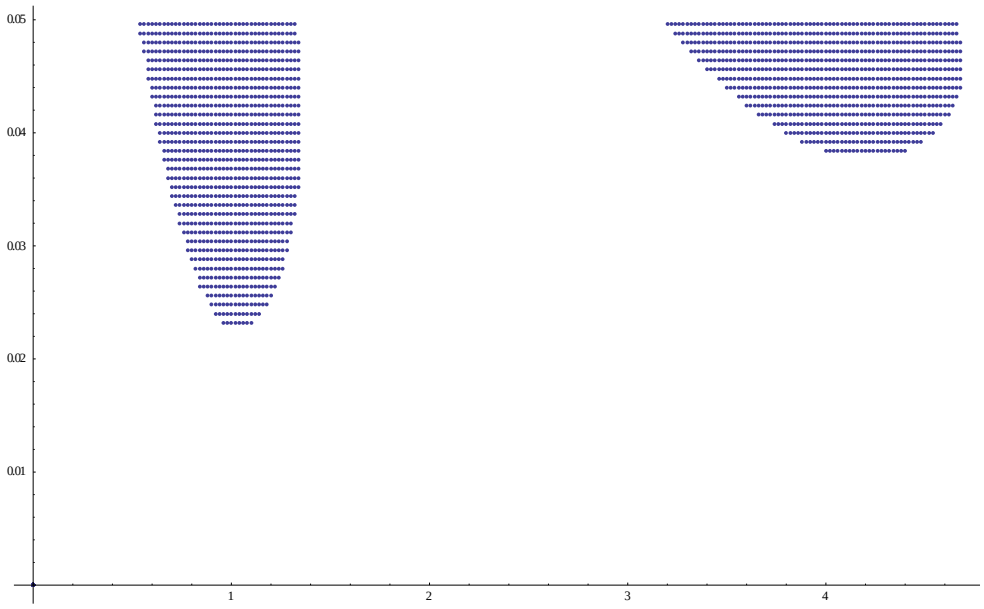

Figure 7.4 Stability chart created for 7 waves and for wavelength=1.25Lship for filter parameter=0.05.

[2] 0.3 radians=17.18 degrees

8. CHAPTER EIGHT: APPLICATION OF THE PROCESS

8.1 Under study ship's characteristics

The application of the methodology mentioned in the previous chapters will use as sample ship the post panamax containership of Table 6.1. It is reminded that the main particulars of this ship are:

Length overall 250.000 m

Length between perpendiculars 238.350 m

Breadth (moulded) 37.300 m

Depth (moulded) 19.600 m

Design draught (moulded) 11.500 m

Freeboard draught (moulded) 12.500 m

Displacement at Td = 11.500 m 68014 t

Displacement at Tscntl = 12.500 m 75729 t

We will examine the Full Load Departure condition of the ship for the selected loading case LC-18 with characteristics:

Loading Case (LC)	Homogenous Weight (t/TEU)	Draft (m)	Initial Metacentric Height GMo (m)	Vertical Distance of Centroid KG (m)
18	16	12.517 (Scntl)	1.48	16.21

8.2 GM variations along the wave

As discussed in paragraph 6.5, we produced a formula for the exact calculation of the metacentric height on every position of the ship on the wave. We calculated these variations for several values of wave steepness and for 3 different values of the filter parameter *a* of the wave. It is reminded that the free surface elevation is given by the expression:

$$f(x) = \frac{H}{2} e^{-a\left(x-\frac{n\lambda}{2}\right)^2/\lambda^2} \cos\left(\frac{2\pi x}{\lambda}\right) \tag{8.1}$$

We will examine the GM variation for a wave length equal to 1.25 of the ship's length, which is translated to

$$\lambda = 1.25 L_{OA} = 312.5\ m \tag{8.2}$$

The wave steepness that we consider is ranging from 0.0016-0.0496, meaning that we consider wave heights from 0.5 m to 15.5 m. So, for the three different cases, where *a=0, 0.025, 0.05* respectively, we can see the GM variations along the wave, for a group of 7 waves, for the range of wave steepness in the next figures.

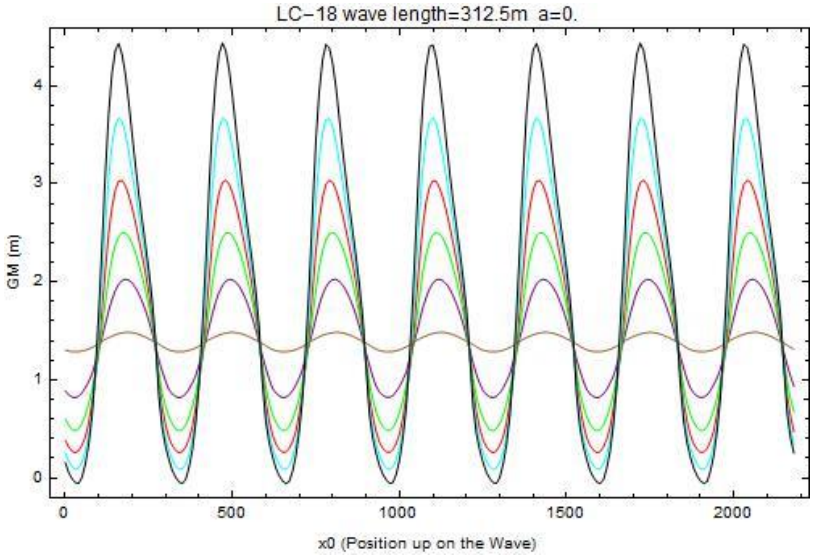

Figure 8.1 GM alteration for a=0 (regular waves).

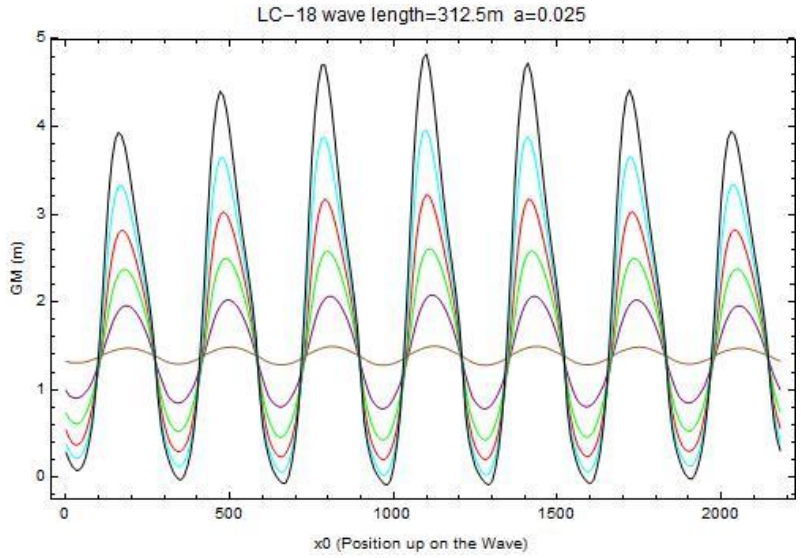

Figure 8.2 GM alteration for a=0.025.

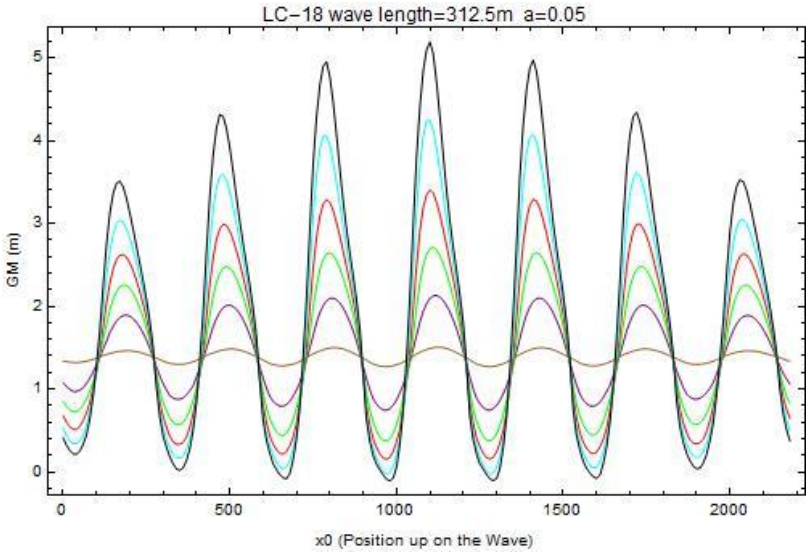

Figure 8.3 GM alteration for a=0.05.

As we can see from the figures Figure 8.1)Figure 8.2)Figure 8.3) the variations of the metacentric height follow the form of the considered wave groups in each situation, as it is expected. Moreover, while the wave steepness increases, which means that the wave height increases because the wave length is constant, we can see that the GM values tend to increase too and have greater differences between maximum and minimum values. Especially, we can see in the last figure that for wave steepness 0.0496 the metacentric height varies from negative values close to 0m(wave crest) to values close to 5m(wave

trough), which is significant if we compare it with the initial GMo=1.48. This considerable alteration of the metacentric height along the wave can lead to the development of parametric rolling, as discussed in chapter 5.

In order the effect of the filter parameter in the GM variation in the above figures to be well perceived, in the next figure the alteration of the GM along the wave for the same value of wave steepness (0.0496) for the three different values of *a* is shown.

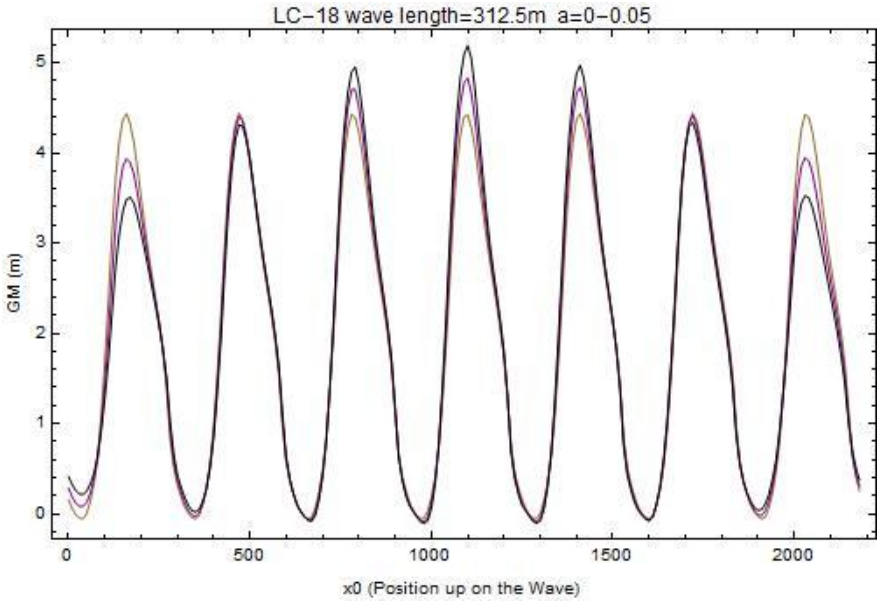

Figure 8.4 GM variation for a=0(brown line), a=0.025(purple line), a=0.05(black line).

From Figure 8.4 it is concluded that, as the value of the filter parameter increases, the metacentric height variation tends to increase too leading possibly[3] to more sensitive in parametric rolling situations.

[3] It will be investigated more detailed in a following chapter.

8.3 Stability charts comparison

The process of the stability chart construction is explained in detail in chapter 7. Several stability charts are shown below and the comparison has to do with:

- the filter parameter *a*
- the wave length *λ*
- the number of waves consisting the group
- changing of wave height and wave length along the group.

8.3.1 Filter parameter's impact

By solving the system of equations which describes fully the problem of the determination of the metacentric height along the wave and by solving differential roll equation (7.1) for a value of *ζ=0.05* and for threshold=0.3 we obtain the following stability charts. It is noted that we examine the LC-18 loading condition for a sequence of 11 waves and for wave steepness ranging from 0.0016-0.0496 for wave length 312.5m.

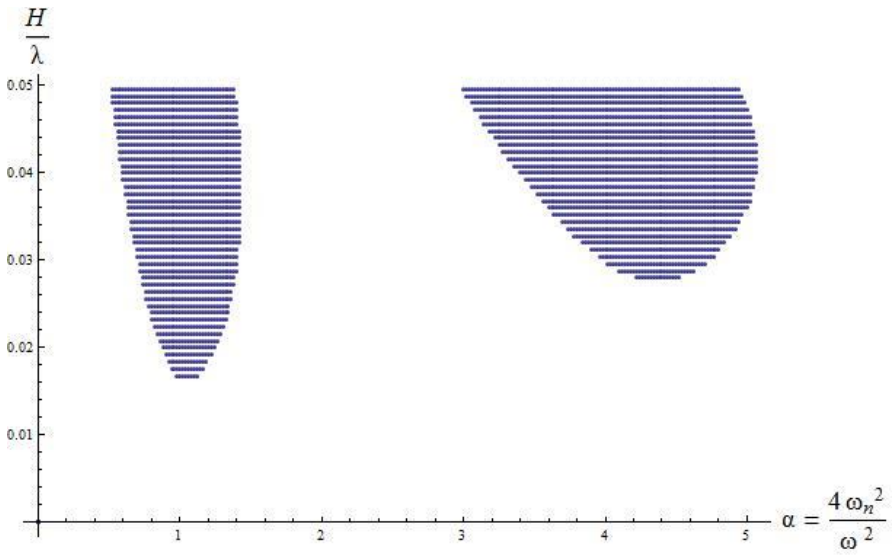

Figure 8.5 Stability chart for a=0.

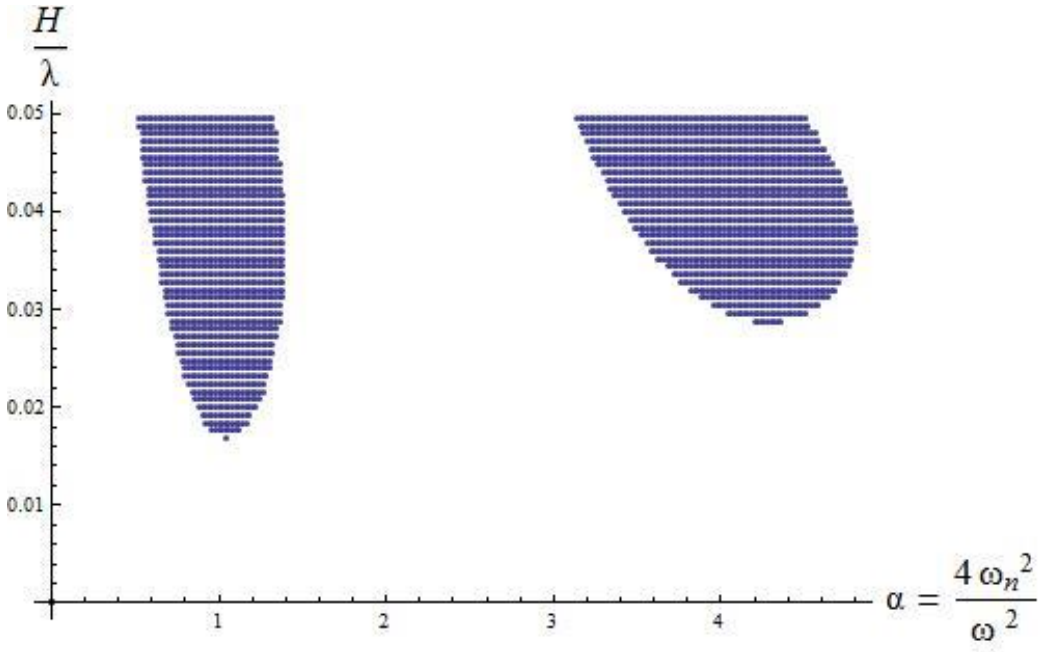

Figure 8.6 Stability chart for a=0.025.

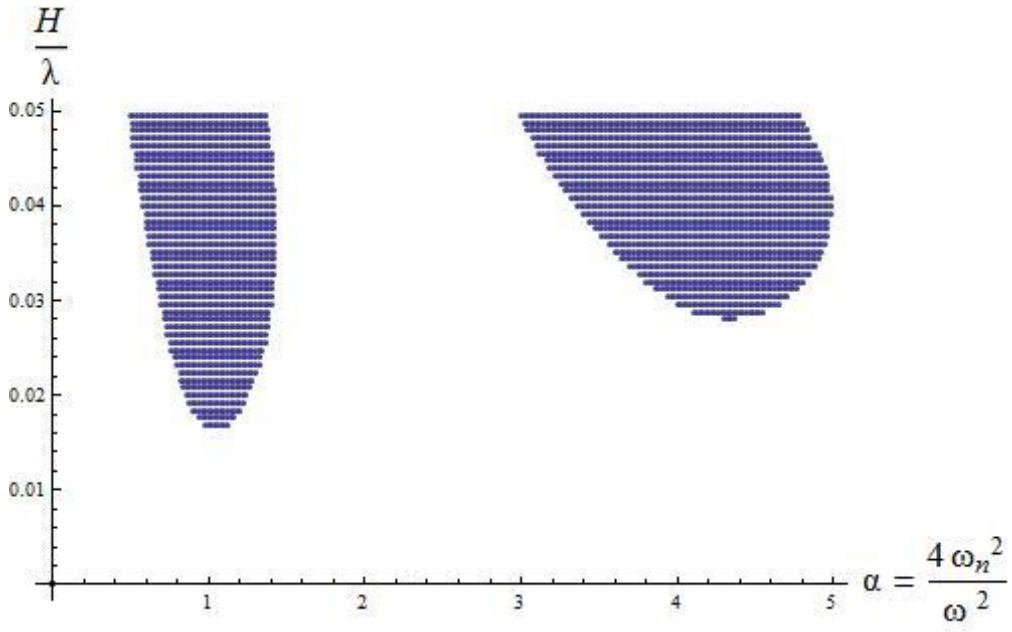

Figure 8.7 Stability chart for a=0.05.

By accumulating the information that the figures Figure 8.5-Figure 8.7 give us, we plot them together in one figure in order useful conclusions to be derived.

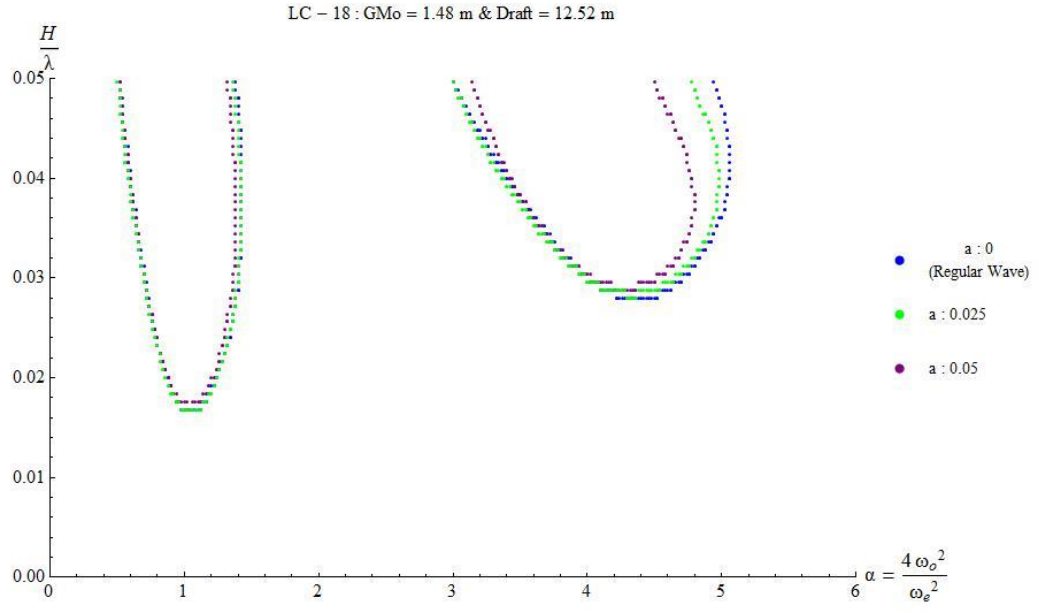

Figure 8.8 Filter parameter's impact on stability charts.

From Figure 8.8 we observe that while in the first region of instability[4] the alteration of the form of the free surface elevation does not affect the result significant, however in the second region it is obvious that the unacceptable situations tend to decrease as the value of the parameter *a* is increasing, i.e. as the wave profile changes from regular to irregular form. As a result, we can say that the hypothesis of regular waves of same amplitude overestimates the sensitivity of the ship on the development of parametric roll, while as we are experimenting with more realistic waves the instability region is decreasing. This comes in contrast to what was expected from the results of the chapter 8.2, where we supposed that the more the waves change form from regular to irregular, which means that the GM alteration becomes greater, the more sensitive in parametric resonance our system will be.

In order to understand the differences numerically, we calculate the percentage of the reduction of instability zones in the second and third case from the first. The second area is reduced by 2.11%, compared to the first, while the third region is reduced by 15.43% compared to the first area.

8.3.2 Comparison by wave length

One of the criteria that must be satisfied in order a ship to develop parametric roll in longitudinal seas, is that the wave length must be approximately equal to the ship's length [2]. Taking the latter condition into consideration, we will investigate the behavior of the under study ship in 3 different wave lengths, i.e. 1L, 1.25L and 1.5L respectively. We will consider group of 11 waves with filter parameter a=0 (regular waves) and wave steepness, damping and threshold as before.

[4] The region around a=1.

1. For $\lambda=1L=250m$ we get

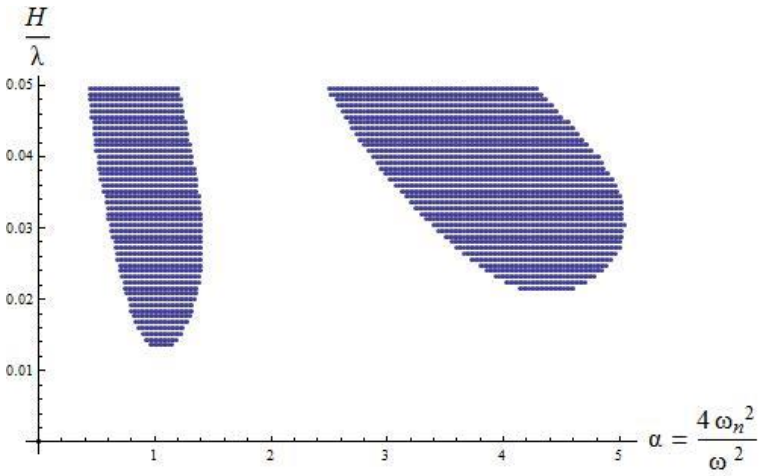

Figure 8.9 Stability chart for $\lambda=250m$

2. For $\lambda=1.25L=312.5m$ we get

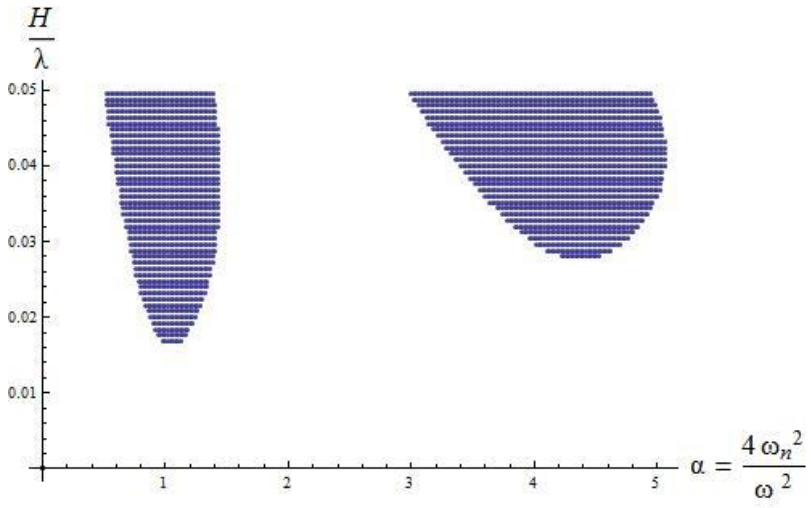

Figure 8.10 Stability chart for $\lambda=312.5m$

3. For $\lambda=1.5L=375m$ we get

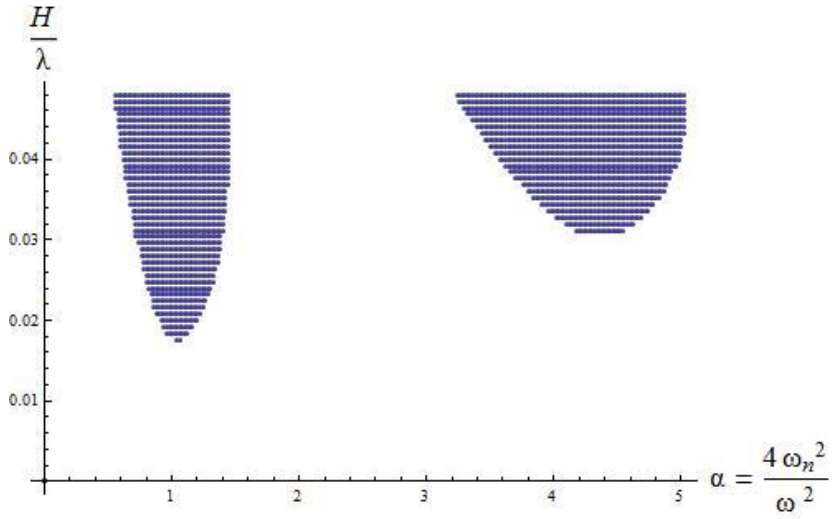

Figure 8.11 Stability chart for *λ=375m*

Again, as before we choose to present these 3 figures into one new figure in order to understand better the transposition of the stability/instability regions of the three cases.

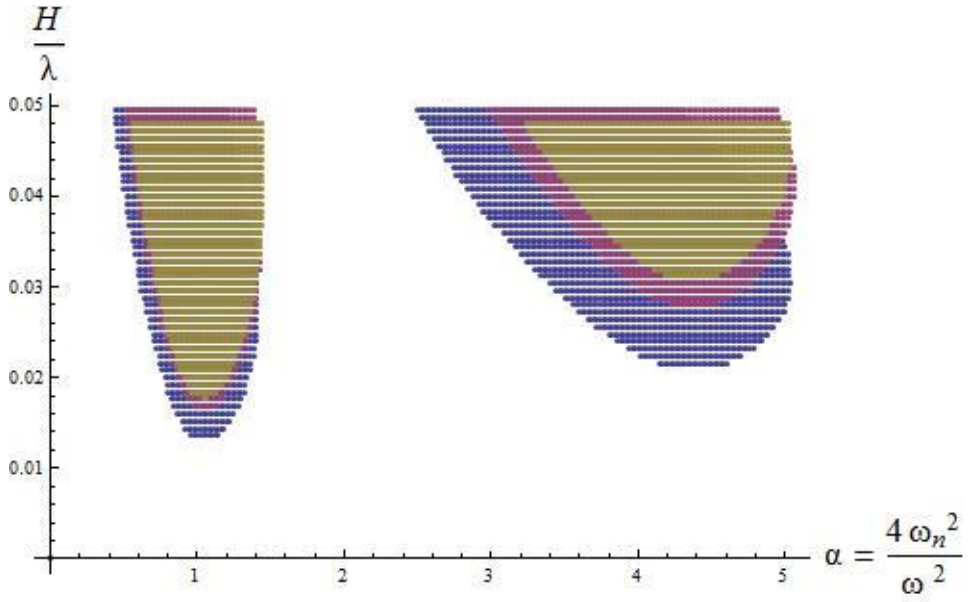

Figure 8.12 Difference in instability areas for *λ=250m(blue), λ=312.5m(purple), λ=375m(brown).*

If we now wish to specify these differences numerically, we need to calculate the areas of each case and compare them. Comparing the first case(*λ=250m*) with the second(*λ=312.5m*), the result is that the difference is 23.88% which means that by increasing the wave length it is observed a reduction of the instability region by almost one quarter of the first. Similarly, the third case is reduced by 41.3% comparing to the first case, which complies with the previous statement. The difference between the second and third case is 22.87%, which means that in general while the wave length increases the instability zones decrease. At this point it is important to remind that the time intervals are the same for the three cases as the factor that changes is the speed.

8.3.3 Comparison by the number of waves

In this last situation we will examine the effect of the number of waves which constitute the group that the ship will encounter. We will study 2 cases: 7 and 11 waves. We will consider the filter parameter *a* to be 0.05 for a wave length of 312.5m and so the stability charts will be:

- For 7 waves

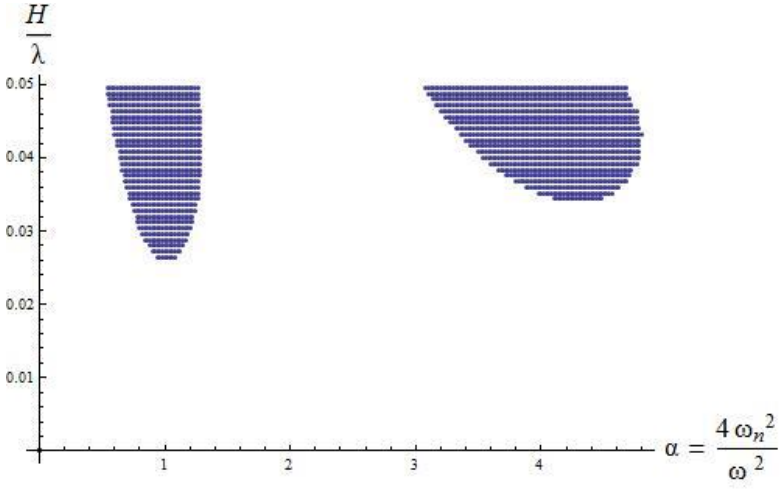

Figure 8.13 Stability chart for 7 waves and a=0.05.

- For 11 waves

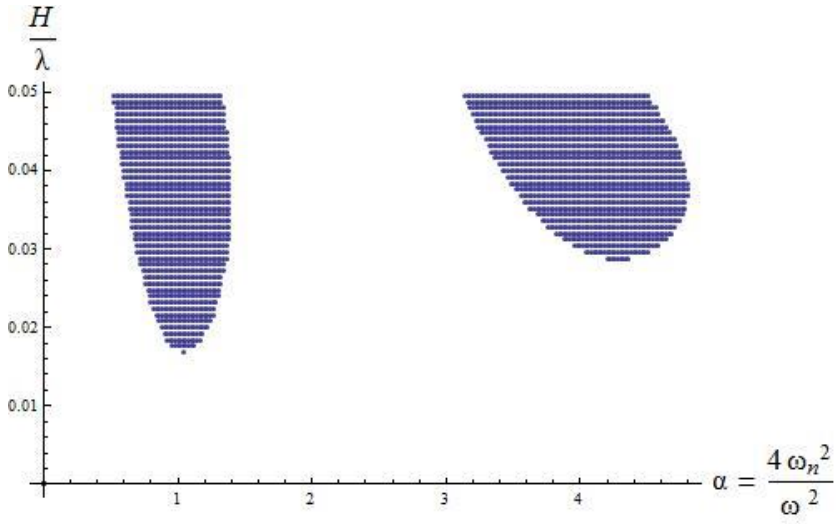

Figure 8.14 Stability chart for 11 waves and a=0.05.

Again these 2 cases in one figure are shown as:

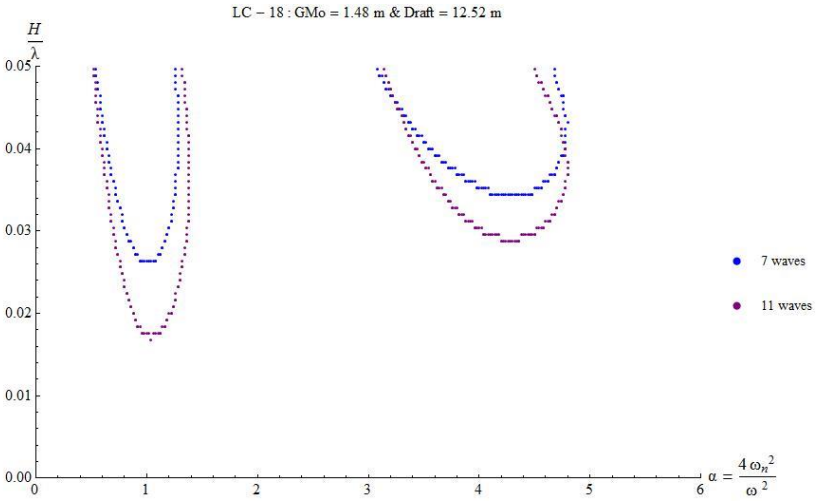

Figure 8.15 Instability zones for 7 and 11 waves.

As it is expected, when we increase the number of waves that the ship will encounter, the probability of occurrence of parametric roll is increased and it can happen for smaller values of the wave steepness and numerically the difference of these two areas is approximately 28.67%.

8.3.4 Investigation of a more complex form (wave height and wave length changing).

So far, we dealt with forms that are by default of the same wave length along the group.
In this chapter, we will focus on the vessel's behaviour when encountering a group where both the wave height and the wave length are not of constant value. Let us consider that this group is consisted of 10 consecutive waves with $\lambda = 312.5m$ each. Following the analysis made in previous chapters, the function that describes the height-varying group is:

$$f(x) = \frac{H}{2} e^{-a\left(x-\frac{10\lambda}{2}\right)^2/\lambda^2} \cos\left(\frac{2\pi x}{\lambda}\right) \quad (8.3)$$

This form is shown in the next figure for a=0.1

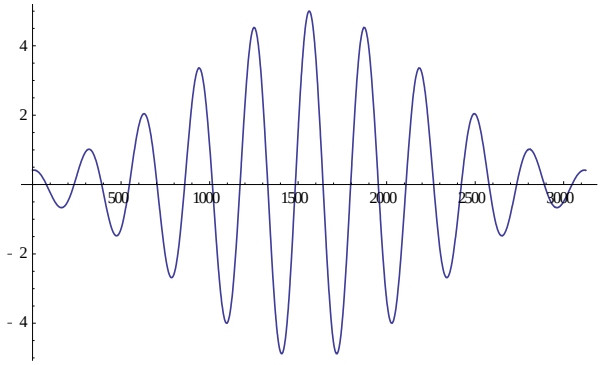

Figure 8.16 Group of 10 height-varying waves.

In order to change the length of each one of these waves, we need to insert a function in (8.3). Let us consider,

$$p(x) = 1 + cLog(x) \quad (8.4)$$

By inserting this function in the first as an exponential, the following function is created:

$$w(x) = \frac{H}{2} e^{-a(x)^{(1+cLog(x))^2}/\lambda^2} \cos\left(\frac{2\pi(x)^{(1+cLog(x))}}{\lambda}\right) \quad (8.5)$$

For a value of c=0.005, the graphical display of this function is shown in the next figure.

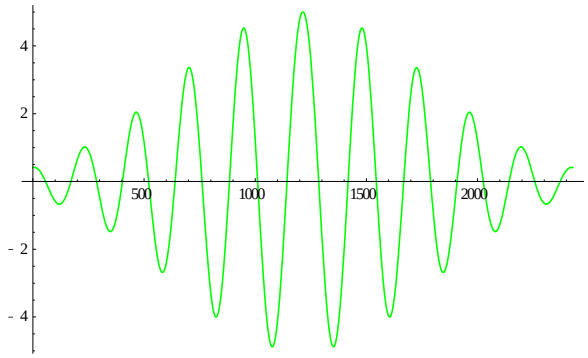

Figure 8.17 Height-changing, length-changing form.

We need to note that the wave length of the first wave is 228.561m, the one of the second wave 232.828m, the third's 238.491m, the fourth's 247.019m and the fifth's 267.321m. The rest of the waves are symmetrically constructed to the first five, so the wave lengths are calculated respectively.

The comparison between these 2 cases is obvious in Figure 8.18.

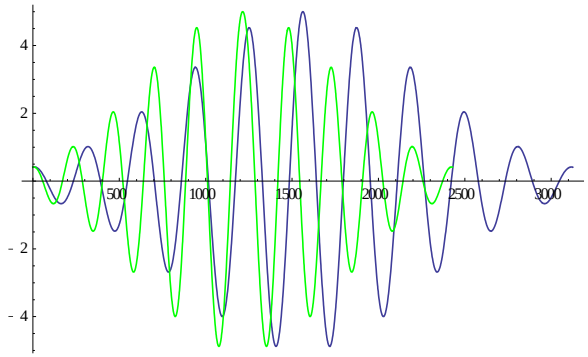

Figure 8.18 Comparison between the two cases

Stability charts will be created for these 2 cases and will be compared to the simple sinusoidal form too. We follow the process that has already been described in previous chapters in order to construct the desired stability charts. After several runs of the program, the result is shown in the following figure.

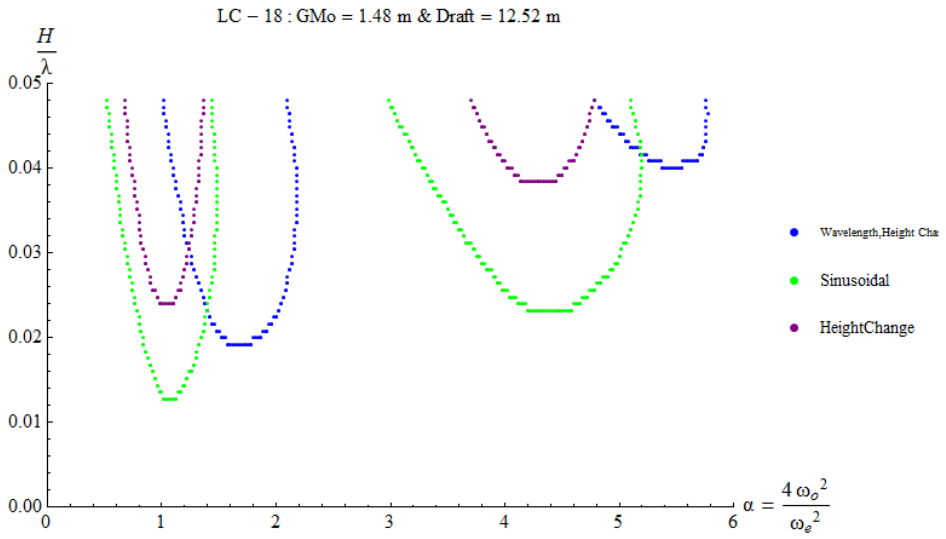

Figure 8.19 Stability charts for three different forms of wave groups.

As we can see in Figure 8.19), the change in the wave lengths along the group causes the transition of the stability chart into areas of lower encounter frequencies region, which is an interesting result.

In the abovementioned analysis, it is obvious that the selected cases are of different total length, which means that the ship needs different time to pass each of these groups.
We can choose to examine these cases for the same time intervals. Because the group *w(x)* (2428.44m) is of less total length than that of *f(x)* (3125m), we will create the stability chart of the second one until the total length of *w(x)* (2428.44 m).

The comparison between the same time intervals for these two examined forms is shown in Figure 8.20).

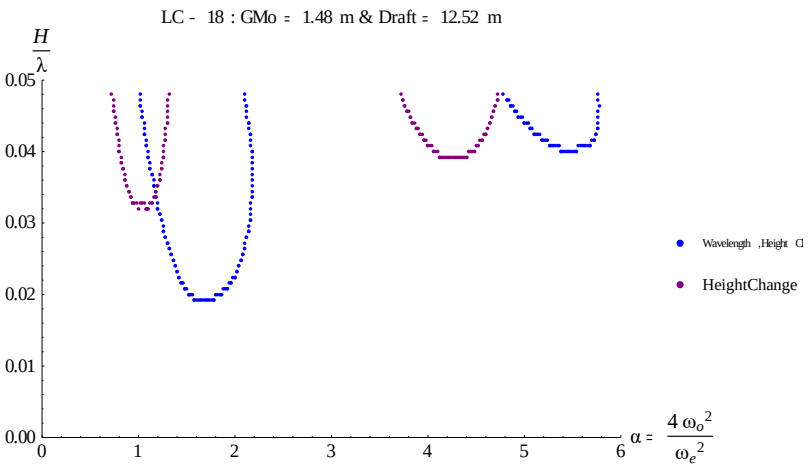

Figure 8.20 Comparison between the 2 selected forms for the same time interval.

The result of the calculations shows that as it was expected, because the time interval is shortened for the height-varying form, which means that the ship does not pass the whole group, the undesirable pairs of wave steepness-encounter frequency are becoming less in the first area of the chart (higher encounter frequencies). However, the second area is almost the same, leading us to consider that this modification of the time does not affect the low encounter frequency zones.

8.4 Forward speed analysis

The importance of the present thesis in practice is revealed in this chapter, where the speed regions which result to instability and parametric roll will be specified in order the captain to have a useful tool to avoid undesired situations while en route. For this reason, we have to distinguish the speed regions that our under study ship can develop during its operation. There are 4 speed regions that will be used for this division:

- 0<Forward speed U(kn)< 15 , which correspond to Super Slow Steaming condition.
- 15<Forward speed U(kn)< 18 , which correspond to Extra Slow Steaming condition.

- 18<Forward speed U(kn)< 21 , which correspond to Slow Steaming condition.
- 21<Forward speed U(kn)< 24 , which correspond to Full Speed condition.

Areas of forward speed greater than 24kn will be considered as unacceptable in the terms of the specific ship, while the Service Speed is given as 21kn.

8.4.1 Comparison with respect to the filter parameter

We will investigate the development of parametric roll in this set of speeds for the stability charts, as they have been produced in previous chapter, for both following and head seas and we will determine the critical wave height for the occurrence of parametric roll in the service speed for both situations. Furthermore, we will compare the areas of the speed regions in the stability charts for the three cases of the filter parameter *a.*

The loading case is as previous the LC-18, the damping coefficient *ζ=0.05* and the threshold is 0.3. A group of 11 waves, each one of them having length 312.5m, will be tested.

1. For the parameter *a=0*, i.e. regular waves, the stability chart is:

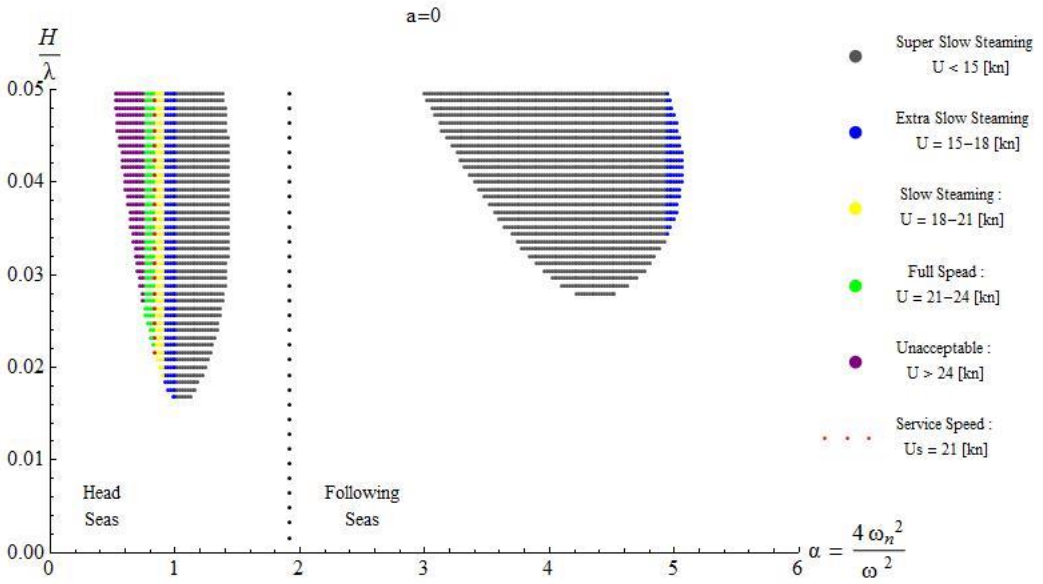

Figure 8.21 Stability chart with respect to ship's forward speed for a=0.

As it is calculated from the code, the minimum value of wave steepness to develop parametric roll in the service speed is 0.0216 which means that the minimum wave height is:

$$H_{min} = 0.0216\lambda = 0.0216 * 312.5 = 6.75\, m$$

And it corresponds only to head seas, as there is no case of service speed associated with following seas.

2. For the parameter a=0.025 the stability chart is:

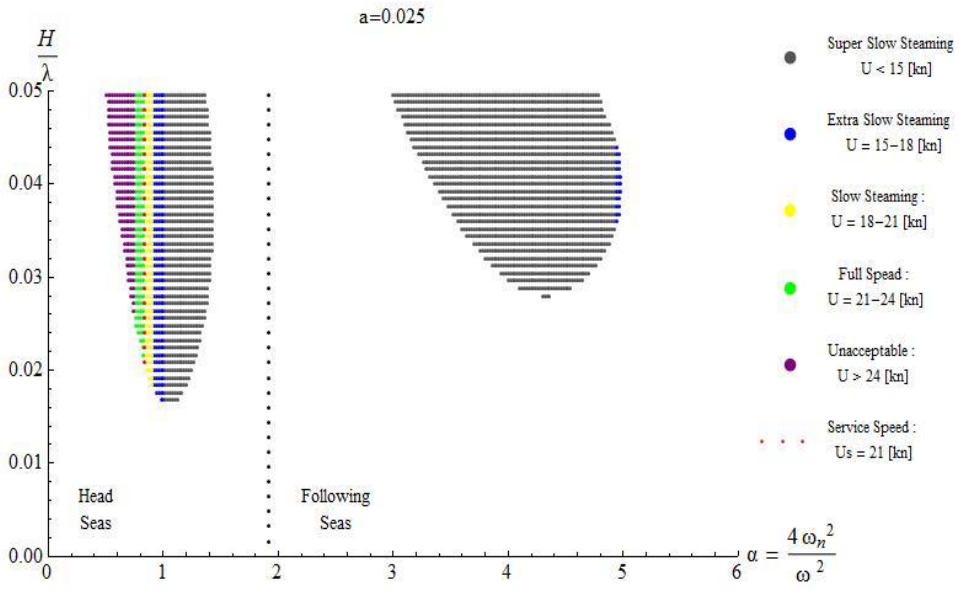

Figure 8.22 Stability chart with respect to ship's forward speed for a=0.025.

Again we need to define the minimum value of wave steepness to develop parametric roll in the service speed and for this case is 0.0208 which translates into:

$$H_{min} = 0.0208\lambda = 0.0208 * 312.5 = 6.5\, m$$

And it corresponds only to head seas, as there is no case of service speed associated with following seas.

3. For the parameter a=0.05 the results are the same as for the regular waves for the minimum wave height to develop parametric roll in the service speed.

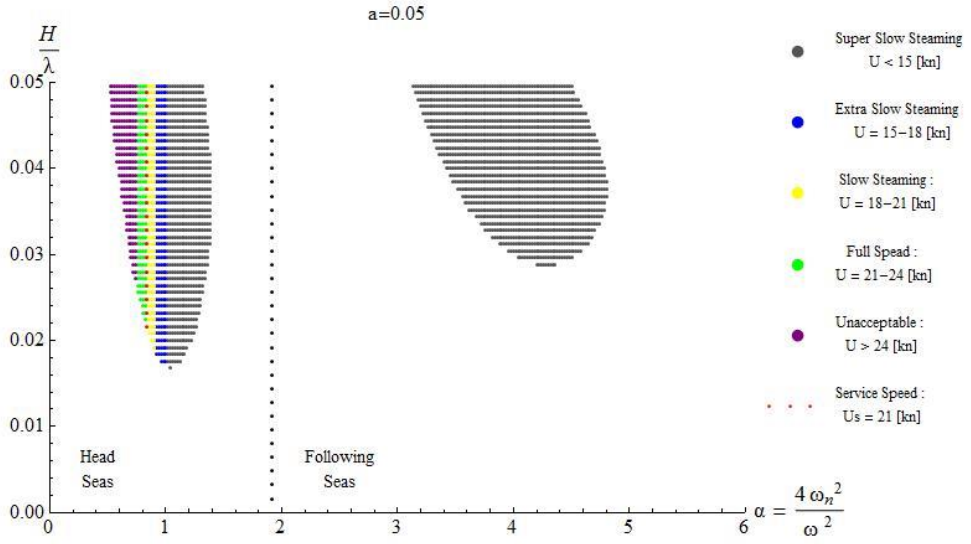

Figure 8.23 Stability chart with respect to ship's forward speed for a=0.05.

We need to have sense of how the alteration of the wave form changes the speed regions of instability. For this reason, we calculated the instability areas for the first two cases of *a=0* and *a=0.025* and separated the speed regions for percentage differences to be extracted. From analysis of the stability charts Figure 8.21),Figure 8.22) the following percentages are resulted:

Super Slow Steaming difference: -1.03 %

Extra Slow Steaming difference: -24.17 %

Slow Steaming difference: 2.6 %

Full Speed difference: 2.22 %

Unacceptable Speed: 9.01 %

The (-) sign means that the instability region is decreased from the first case (regular waves) to the second (*a=0.025)*. From the above percentages it is obvious that the irregularity of the waves contributes to the reduction of the possibility of parametric roll by decreasing the instability region by 24.17% for the Extra Slow Steaming condition, while the

differences for the other regions are not significant. Accordingly, if we wish to compare the regular waves (first case) with the third one, which represents stronger irregularity than the second one, we will follow the same procedure and the results are:

Super Slow Steaming difference: -16.47 %

Extra Slow Steaming difference: -32.78 %

Slow Steaming difference: 0.0 %

Full Speed difference: 0.0 %

Unacceptable Speed: 2.88 %

As it is obvious, the more we move from regular to irregular forms of waves, the more the instability zones in the Super and Extra Slow Steaming are decreased, revealing that the more theoretic approaches of the wave field overestimate the possibilities of occurrence of parametric roll in general for low speeds.

8.4.2 Influence of the number of waves

If we now choose to examine the effect of the number of waves on the minimum value of wave steepness that is needed to develop parametric roll in the service speed, we have to create the stability chart for 7 waves and for 2 values of the filter parameter as previous.

1. For the parameter a=0, i.e. regular waves, the stability chart is:

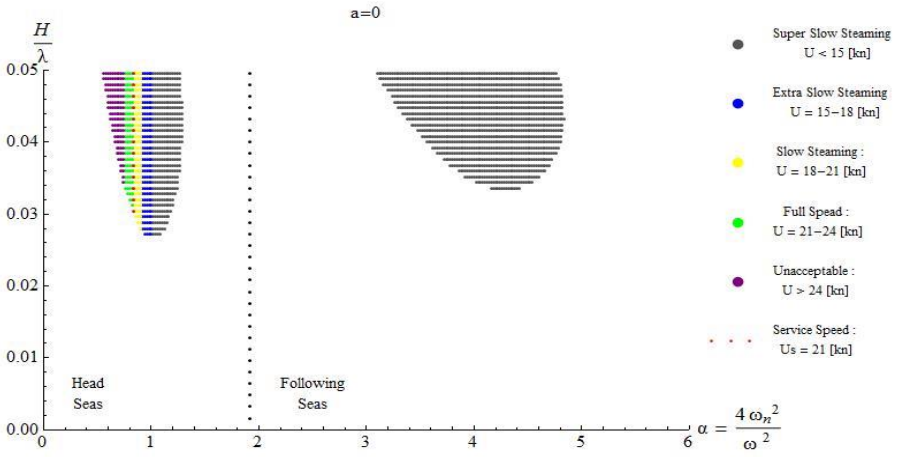

Figure 8.24 Stability chart of 7 waves with respect to ship's forward speed for a=0.

The minimum value of wave steepness to develop parametric roll in the service speed is 0.0304 which means that the minimum wave height is:

$$H_{min} = 0.0304\lambda = 0.0304 * 312.5 = 9.5\, m$$

And it corresponds only to head seas, as there is no case of service speed associated with following seas.

2. For the parameter a=0.025 the stability chart is:

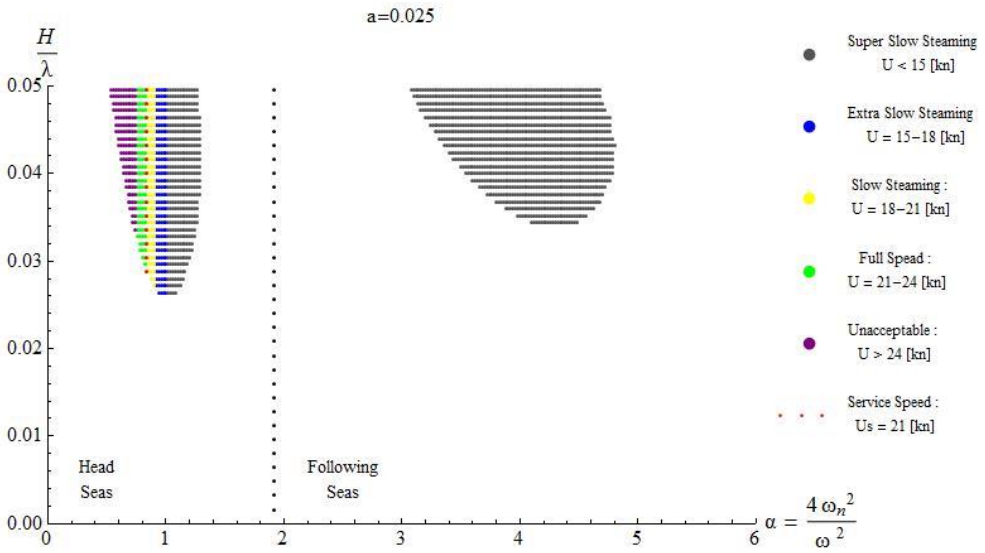

Figure 8.25 Stability chart of 7 waves with respect to ship's forward speed for a=0.025.

In this case the minimum wave steepness in order to develop parametric roll in the service speed is 0.0296 which translates into:

$$H_{min} = 0.0296\lambda = 0.0296 * 312.5 = 9.25\, m$$

Our assumption that by increasing the number of consecutive waves that the ship will encounter is increasing the possibility of development of parametric roll is proven right, as for the group of 11 waves the minimum wave height is 6.75 and 6.5, for the 2 first cases of

the filter parameter, while for the group of the 7 waves the minimum wave height increases dramatically to 9.5 and 9.25 respectively. The percentage of decrease of the minimum height is then approximately 29% from the 7 waves to the 11 waves which is a significant as well as expected difference.

8.4.3 Comparison of loading cases

So far, we have investigated the loading case LC-18, where the initial metacentric height is relatively adequate. The numerical solutions of the differential roll equation have not shown any incident of development of parametric roll in the service speed in following seas. This does not mean that parametric roll cannot happen in following seas though. If we choose to examine a loading condition of smaller marginally adequate metacentric height, then cases of occurrence of parametric roll in both wave direction scenarios will be revealed. For this reason, we choose from the stability booklet of the under study ship to test the loading case LC-15 with the following characteristics:

Loading Case (LC)	Homogenous Weight (t/TEU)	Draft (m)	Initial Metacentric Height GMo (m)	Vertical Distance of Centroid KG (m)
15	12	12.517 (Scntl)	0.494	17.17

For the selected loading case we will construct the stability chart for regular wave form *(a=0)* for a group of 11 waves of $\lambda=312.5m$ each, with the all other factors to be as in the previous simulations. In the next figure the speed regions for instability are shown for the LC-15.

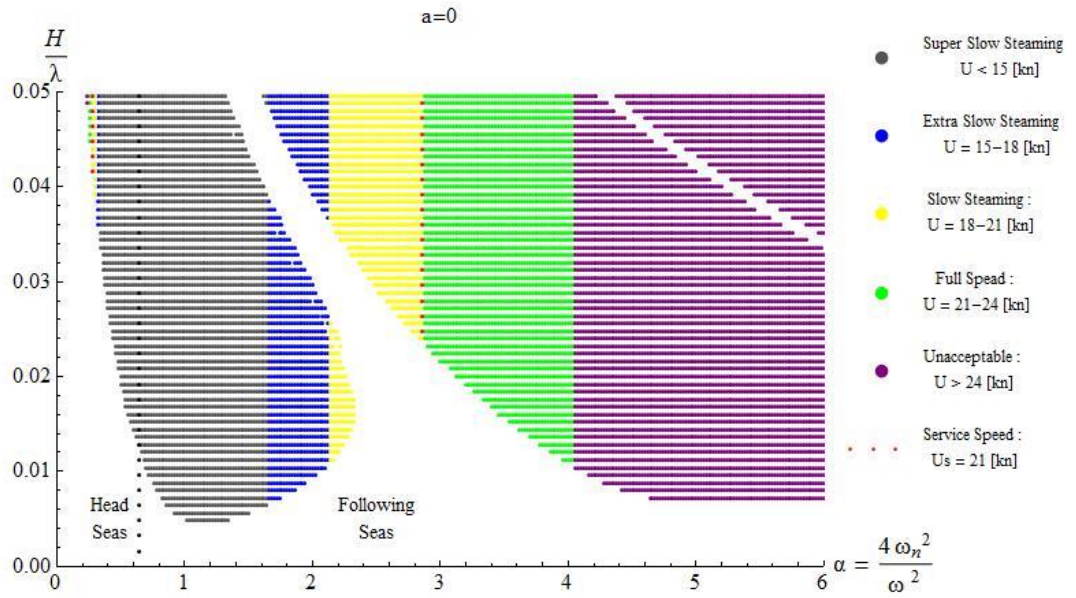

Figure 8.26 Stability chart with respect to ship's forward speed for the LC-15 and a=0.

We can see now that due to the small initial metacentric height, the areas of instability are quite larger than these of the LC-18. We also notice the development of parametric roll for both head and following seas in the service speed (dotted line) and specifically:

The minimum wave steepness needed to develop parametric roll in head seas is 0.0416, which means minimum wave height

$$H_{min} = 0.0416\lambda = 0.0416 * 312.5 = 13\ m$$

The minimum wave height for following seas is spotted in the place of wave steepness 0.0248, which means

$$H_{min} = 0.0248\lambda = 0.0248 * 312.5 = 7.75\ m$$

If we compare the figures Figure 8.21)Figure 8.26) we can see that while for the second case (LC-15) the instability area is greater than the first one (LC-18), the minimum required wave height in head seas in order to develop parametric roll in the service speed is almost doubled (6.75m to 13m). This shows that although we have smaller value of GM in the second case, we have better behaviour in the service speed for head sea scenarios.

9. CHAPTER NINE: CONCLUSIONS AND FURTHER STUDY

The present thesis dealt with the dynamic stability of ships under the scope of parametric roll. For this purpose a code in Wolfram Mathematica environment was constructed which included a SDOF model of the differential roll equation with linear damping and the restoring term (GM) was calculated numerically along the wave. This direct calculation of the metacentric height on the wave differs from the conservative sinusoidal form of the restoring term consideration of past studies and is approaching the reality in a better way. From the several simulations of the method and the creation of the corresponding stability charts, it is concluded that the method is capable of capturing parametric resonance phenomena, such as parametric rolling. We chose to investigate this phenomenon using a height varying group of waves, thus considering the wave field irregular. Many aspects of the problem were touched such as:

- The effect the change of the wave height along the wave group has into the stability and sensitivity to parametric roll.
- The importance of the wave length λ and how the stability/instability zones are affected by wave groups with different values of wave lengths of each wave.
- How the number of waves that consist the wave group influences the behaviour of the vessel and the stability charts.
- The effect of the change of both the wave height and wave length along the wave in the stability charts.
- The role of the loading condition and moreover the initial metacentric height have in the interaction between the ship and the sea and the development of roll angles.

Through analysis of the abovementioned aspects and by comparing different cases as stated in chapter 8 we were able to come to very useful conclusions which are the following:

- As long as it concerns the wave form, the results show that by moving from a strictly regular form of the free surface elevation *(a=0)* to more realistic approaches of the wave field *(a=0.025,a=0.05)*, by keeping the total wave energy equal for all the three cases, the instability zones tend to decrease mainly in the area of fundamental resonance. The differences in the area of principal resonance are insignificant. This

decrease happens even though the fluctuations of the metacentric height in irregular wave forms are greater than these of the regular waves.

- The wave length is a factor of great importance when investigating the dynamic stability of a ship. The results of the analysis of three different sets of wave groups with three different wave lengths reveal that the more the wave length is increasing, the more resistance of the ship in parametric roll is increasing too and the stability charts are moving upwards. It is noted that as a reference, the time intervals are the same for these three cases and the speed is changing.
- It was expected, but we verified that the number of the waves that may constitute a wave group is a major factor in the parametric behavior of the vessel. By comparing two different sets, with 7 and 11 waves respectively, of waves groups, the increase of the number of waves increases the possibility of occurrence of parametric roll in smaller wave steepness.
- We examined the influence of the filter parameter on the stability charts with respect to the ship forward speed regions for a set of 4 possible speed areas the ship may develop during its lifetime. The analysis proved that the irregularity of the waves, which is a more realistic consideration, reduces the possibility of development of parametric roll phenomenon in slow speed regions dramatically.
- Again, if we choose to study the factor of the number of waves in the group, as the latter increases the minimum wave height in order to develop parametric roll in the service speed is decreased making the vessel more prone to dynamic instability phenomena.
- Last but not least, a comparison between two different loading cases, one with adequate initial metacentric height and the other with marginal, showed that as the metacentric height is decreasing areas of parametric rolling in the service speed are showing in following seas too, and not only in head seas. Moreover, as the initial metacentric height is decreasing, higher values of wave height are required in order to develop parametric roll in head seas even though the stability is reduced.

The method and the conclusions are moving towards the scope of a more realistic approach of the phenomenon, but much more can be done to develop this work such as:

- A more detailed construction of wave groups not only of height varying, but also of wave length varying form which is a step closer to real sea states.

- Further analysis by considering the free surface elevation as a stochastic process and by inserting the spectra of ocean waves into the calculations.
- Simulations by using a 3-DOF model of coupled motions of roll, pitch and heave in order to include the influence of all motion in the development of parametric roll.
- Consideration of the damping as nonlinear function rather than the linear which was used in the present thesis.

References

[1] Belenky, V., De Kat, J.O., Umeda, N., (2008). "Towards performance-based criteria for intact stability", Marine Tech., 45(2):101– 123.

[2] France, W. M, M. Levadou, T. W. Treakle, J, R. Paulling, K. Michel & C. Moore (2001). "An Investigation of Head-Sea Parametric Rolling and its Influence on Container Lashing Systems", SNAME Annual Meeting 2001 Presentation.

[3] IMO-MSC/Circ. 707, (1995). "Guidance to the master for avoiding dangerous situations in following and quartering seas".

[4] IMO-MSC.1/Circ.1228, (2007). "Revised Guidance to the master for avoiding dangerous situations in adverse weather and sea conditions".

[5] Peters, W., Belenky, V., Bassler, C., Spyrou, K.J., Umeda, N., Bulian, G., Altmayer, B., (2011). "The second generation of Intact stability criteria: an overview of development", Trans. Soc. Nav. Arch. Mar. Eng., 119:225–264.

[6] Umeda, N., (2013). "Current status of second generation intact stability criteria development and some recent efforts", 13th International Ship Stability Workshop, 138–157, Brest, France.

[7] http://www.bizjournals.com

[8] Faraday, M., (1831). "On a peculiar class of acoustical figures; and on certain forms assumed by groups of particles upon vibrating elastic surfaces," Philosophical Transactions of the Royal Society of London, 121:299–340.

[9] Chladni, E., (1787). "Discoveries in the Theory of Sound", Leipzig, Germany.

[10] Melde, F., (1859). "On the excitation of standing waves on a string", Ann. Phys. Chem. 109, 193.

[11] Mathieu, E., (1868). "Memoire sur Le Mouvement Vibratoire d'une Membrane de Forme Elliptique," Journal de Mathématiques Pures et Appliquées, 13:137-203.

[12] Froude, W., (1861). "On the rolling of ships", Transaction of the Institution of Naval Architects, 2: 180–227.

[13] Paulling, J. R., (2011)."Parametric Rolling of Ships, Then and Now", Contemporary Ideas on Ship Stability and Capsizing in Waves Fluid Mechanics and Its Applications, 97: 347-360.

[14] Spyrou, K.J, (2006). "Ευστάθεια Διατοιχισμού Πλοίου και Υπόβαθρο Κανονισμών", Σημειώσεις Μαθήματος, National Technical University of Athens, Athens, Greece.

[15] Paulling, J. R., Rosenberg, R. M., (1959). "On Unstable Ship Motions Resulting from Nonlinear Coupling", Journal of Ship Research, 3(1):36–46.

[16] Galeazzi, R., (2009). "Autonomous Supervision and Control of Parametric Roll Resonance", PhD thesis, 29-45, Technical University of Denmark, Copenhagen, Denmark.

[17] Spyrou, K.J, (2000). "Design Against parametric Instability in following seas", Ocean Engineering, 27:625–653.

[18] Lloyd's Register, (2003). "Head-sea parametric rolling of container ships", Marine Service Information Sheet.

[19] Shin, Y., Belenky, V.L., Paulling, J.R., Weems, K.M., Lin, W.M., (2004). "Criteria for parametric roll of large containerships in head seas", SNAME Annual Meeting.

[20] Spyrou, K.J, (2005). "Design Criteria for parametric rolling", Oceanic Engineering International, 9(1):11-27.

[21] Spyrou, K.J, Themelis, N., Niotis, S., (2007). "Probabilistic assessment of parametric rolling: comparative study of detailed and simplified models", Proceedings of the 9th International Ship Stability Workshop, National Technical University of Athens, Athens, Greece.

[22] Themelis, N., Spyrou, K.J, (2008). "Probabilistic Assessment of Ship Stability Based on the Concept of Critical Wave Groups", Proceedings of the 10th International Ship Stability Workshop, National Technical University of Athens, Athens, Greece.

[23] Spyrou, K.J, Tigkas, I., Scanferla, G., Pallikaropoulos, N., Themelis, N., (2008). "Prediction potential of the parametric rolling behavior of a post-panamax containership", Ocean Engineering, 35: 1235–1244.

[24] Shigunov, V., el Moctar, O., Rathje, H. (2009). "Conditions of Parametric Rolling", Proceedings of the 10th International Conference on Stability of Ships and Ocean Vehicles, St. Petersburg, Russia.

[25] Hong, S.Y., Yu, H.C., Kim, S., Sung, H. G., (2009). "Investigation of parametric roll of a container ship in irregular seas by numerical simulation", Proceedings of the 10th International Conference on Stability of Ships and Ocean Vehicles, 549-558, St. Petersburg, Russia.

[26] Belenky, V., Bassler, C., (2010). "Procedures for Early-Stage Naval Ship Design Evaluation of Dynamic Stability: Influence of the Wave Crest". Naval Engineers Journal, 122(2):93–106.

[27] Silva, S.R, Turk, A., Soares, C.G., Prpic-Orsic, J., (2010). "On the Parametric Rolling of Container Vessels", Technical Paper, 61(4):347-358.

[28] Rosen, A., Huss, M., Palmquist, M., (2012). "Experience from Parametric Rolling of Ships", Springer, 147-165.

[29] Dousia, G., (2015). "Numerical Analysis of Parametric Roll Resonance of a Containership Sailing in Nonlinear, Longitudinal Seas", Diploma Thesis, National Technical University of Athens, Athens, Greece.

[30] Kontolefas, I., (2012). "Αριθμητική μελέτη του φαινομένου Surf-Riding σε ακολουθούντες κυματισμούς ανωτέρας τάξης", Diploma Thesis, National Technical University of Athens, Athens, Greece.

[31] Craik, A. D. D., (2004). "The origins of water wave theory", Annual Review of Fluid Mechanics, 36:1-28 , University of St. Andrews, St. Andrews, United Kingdom.

[32] Ochi, M. K., (1998). "Ocean Waves: The Stochastic Approach", Cambridge University Press, 13-17, Cambridge, United Kingdom.

[33] Journée, J.M.J., Pinkster, J., (2002)."Introduction in Ship Hydromechanics", Delft University of Technology, 31-34, Delft, Netherlands.

[34] Tzampiras, J., (2015). "Υδροστατική και Ευστάθεια Πλοίου ", 8-10, Athens,Greece.

[35] Levadou, M., Gaillarde, G., (2003). "Operational guidance to avoid parametric roll", Proc. RINA Int. Conf. on Design and Operation of Container Ships, 75-86.

[36] https://www.sec.gov/

[37] Galeazzi, R., Blanke, M., Poulsen, N. K., (2011). "Early detection of parametric roll resonance on container ships", Technical report, Technical University of Denmark, Copenhagen, Denmark.

[38] http://www.cargolaw.com/

[39] Kreuzer, E., Sichermann, W., (2006). "The Effect of Sea Irregularities on Ship Rolling", 8(3):26-34, Hamburg University of Technology, Hamburg, Germany.

[40] Perez, N., Sanguinetti, C., (2006). "Scale model tests of a fishing vessel in roll motion- Parametric resonance", Síntesis Tecnológica. 3(1):33-37,Austral University of Chile, Valdivia, Chile.

[41] Galeazzi, R., Blanke, M., (2007). "On the feasibility of stabilizing parametric roll with active bifurcation control", Conference on Control Applications in Marine Systems, IFAC.